Progress in Oceanography 159 (2017) 154–177

Contents lists available at ScienceDirect

Progress in Oceanography

journal homepage: www.elsevier.com/locate/pocean

The elemental stoichiometry (C, Si, N, P) of the Hebrides Shelf and its role in carbon export

Stuart C. Painter[a,*], Susan E. Hartman[a], Caroline Kivimäe[a], Lesley A. Salt[b], Nicola M. Clargo[c], Chris J. Daniels[a], Yann Bozec[b], Lucie Daniels[a,d], Stephanie Allen[a,d], Victoria S. Hemsley[a,d], Grigorios Moschonas[e], Keith Davidson[e]

[a] National Oceanography Centre, European Way, Southampton SO14 3ZH, UK
[b] Sorbonnes Universités, UPMC Univ Paris 06, CNRS, UMR 7144 Adaptation et Diversité en Milieu Marin, Station Biologique de Roscoff, Place Georges Teissier, 29680 Roscoff, France
[c] NIOZ Royal Netherlands Institute for Sea Research, P.O. Box 59, 1790 AB Den Burg, Texel, The Netherlands
[d] Ocean and Earth Science, University of Southampton, National Oceanography Centre, European Way, Southampton SO14 3ZH, UK
[e] Scottish Association for Marine Science, Scottish Marine Institute, Oban PA37 1QA, UK

ARTICLE INFO

Keywords:
Stoichiometry
Dissolved nutrients
Particulate organic matter
NW European shelf sea

ABSTRACT

A detailed analysis of the internal stoichiometry of a temperate latitude shelf sea system is presented which reveals strong vertical and horizontal gradients in dissolved nutrient and particulate concentrations and in the elemental stoichiometry of those pools. Such gradients have implications for carbon and nutrient export from coastal waters to the open ocean. The mixed layer inorganic nutrient stoichiometry shifted from balanced N:P in winter, to elevated N:P in spring and to depleted N:P in summer, relative to the Redfield ratio. This pattern suggests increased likelihood of P limitation of fast growing phytoplankton species in spring and of N limitation of slower growing species in summer. However, as only silicate concentrations were below potentially limiting concentrations during summer and autumn the stoichiometric shifts in inorganic nutrient N:P are considered due to phytoplankton nutrient preference patterns rather than nutrient exhaustion. Elevated particulate stoichiometries corroborate non-Redfield optima underlying organic matter synthesis and nutrient uptake. Seasonal variation in the stoichiometry of the inorganic and organic nutrient pools has the potential to influence the efficiency of nutrient export. In summer, when organic nutrient concentrations were at their highest and inorganic nutrient concentrations were at their lowest, the organic nutrient pool was comparatively C poor whilst the inorganic nutrient pool was comparatively C rich. The cross-shelf export of these pools at this time would be associated with different efficiencies regardless of the total magnitude of exchange. In autumn the elemental stoichiometries increased with depth in all pools revealing widespread carbon enrichment of shelf bottom waters with P more intensely recycled than N, N more intensely recycled than C, and Si weakly remineralized relative to C. Offshelf carbon fluxes were most efficient via the inorganic nutrient pool, intermediate for the organic nutrient pool and least efficient for the particulate pool. N loss from the shelf however was most efficient via the dissolved organic nutrient pool. Mass balance calculations suggest that 28% of PO_4^{3-}, 34% of NO_3^- and 73% of Si drawdown from the mixed layer fails to reappear in the benthic water column thereby indicating the proportion of the nutrient pools that must be resupplied from the ocean each year to maintain shelf wide productivity. Loss to the neighbouring ocean, the sediments, transference to the dissolved organic nutrient pool and higher trophic levels are considered the most likely fate for these missing nutrients.

1. Introduction

The coastal ocean is responsible for 10–20% of global marine primary production, 8–15% of net oceanic CO_2 uptake, and ~40% of global particulate carbon sequestration yet covers only ~7% of global ocean area (Wollast, 1998; Thomas et al., 2004; Muller-Karger et al., 2005; Simpson and Sharples, 2012; Chen et al., 2013; Schlesinger and Bernhardt, 2013; Laruelle et al., 2014). Shallow coastal seas therefore play a disproportionately important role in many aspects of the global carbon cycle (Liu et al., 2010; Wong et al., 2014). The coastal ocean is

* Corresponding author.
E-mail address: stuart.painter@noc.ac.uk (S.C. Painter).

http://dx.doi.org/10.1016/j.pocean.2017.10.001
Received 12 December 2016; Received in revised form 10 July 2017; Accepted 3 October 2017
Available online 05 October 2017

also changing rapidly in response to multiple stressors and understanding of its role in the global carbon cycle remains incomplete (Bauer et al., 2013; Regnier et al., 2013; Wong et al., 2014).

As a net sink for atmospheric CO_2 the coastal ocean removes 0.2–0.4 Pg C annually (Chen et al., 2013; Laruelle et al., 2014). Ultimately this carbon, along with carbon transferred to the benthic waters of the shelf via the biological carbon pump, is exported offshelf into the ocean interior forming the continental shelf pump with only a small fraction buried in shelf and upper continental slope sediments (Mitchell et al., 1997; de Haas et al., 2002; Thomas et al., 2005). It is generally accepted that the continental shelf pump must operate at a similar magnitude to the net atmospheric CO_2 sink in order for the latter sink to occur at all. However, whether the continental shelf pump operates under a fixed or variable stoichiometry relative to the oceanic mean has interesting consequences for the long-term biological productivity of the shelf. If, for example, the net offshelf carbon flux is associated with a fixed carbon to nitrogen (C:N) or carbon to phosphorous (C:P) ratio that is equal to the oceanic inflow a persistent net carbon export due to atmospheric inputs would lead to long-term N and P limitation on the shelf. Consequently, riverine N and P input, atmospheric N deposition and biological N_2 fixation assume a greater importance for balancing shelf productivity nutritional requirements. Alternatively, if there is plasticity in C:N or C:P then a net offshelf carbon flux can be sustained by internal biogeochemical processes that elevate C:N or C:P in the outflowing waters relative to oceanic waters flowing onto the shelf. Clearly, which of these two scenarios is correct is important to understand as a fixed ratio assumption may require the identification of additional nutrient sources to support shelf wide productivity, whilst the variable ratio assumption does not. An answer to this question can subsequently inform the wider debate about the internal biogeochemical functioning of shelf sea systems, numerical model development, and whether there are missing nutrient source terms or not.

Here we demonstrate that a critical component of the coastal ocean's ability to export and potentially sequester carbon in the adjacent ocean is strong plasticity in elemental ratios in both dissolved and particulate pools driven by biological and physicochemical processes. Consequently, greater awareness of the importance of seasonally variable stoichiometry is recommended for future coastal ocean studies.

2. Methods

2.1. Hebrides Shelf

The Hebrides Shelf (~55–60°N, 6–10°W), part of the larger Northwest European Shelf, was sampled in October and November 2014. Six cross-shelf transects were conducted extending from the mid-shelf past the shelf break and out into the open North Atlantic Ocean (Fig. 1a). Water samples were collected from between 5 and 24 depths for a range of analyses including dissolved inorganic nutrients, dissolved oxygen, dissolved inorganic carbon (DIC), and particulate fractions, including particulate organic carbon (POC), particulate organic nitrogen (PON), particulate organic phosphorous (POP), particulate inorganic carbon (PIC), and biogenic silica (bSi).

Nutrient samples were collected in sterile 25 ml plastic vials and analysed immediately using a Skalar Sanplus autoanalyser, common methodologies (Kirkwood, 1996; Hydes et al., 2010) and internationally certified reference materials (http://www.scor-int.org/SCOR_WGs_WG147.htm).

Dissolved oxygen concentrations were measured in duplicate with the Winkler whole bottle titration method (Langdon, 2010). Up to 12 depths were sampled at each station with measurement accuracy estimated to be ± 0.31 μmol L^{-1}. Apparent oxygen utilization (AOU) rates were calculated as the difference between saturated oxygen concentrations calculated from in-situ temperature and salinity and measured dissolved oxygen concentrations (e.g. Clargo et al., 2015).

DIC samples were collected and measured following best practice guidelines (Dickson et al., 2007). 0.6 L water samples were collected in borosilicate glass bottles with plastic caps and analysed immediately on-board in a temperature controlled container laboratory using two VINDTA 3C instruments. All analyses were conducted using certified reference material (batch 140) and the data is available via Hartman et al. (2017). Note that in the text below DIC concentrations may be reported with dual units of μmol kg^{-1} and μmol L^{-1}. This was due to aspects of the following analysis being possible only with data reported in base units of μmol L^{-1}. DIC concentrations were converted from the preferred units of μmol kg^{-1} to μmol L^{-1} using a density conversion factor based on the sample salinity and analytical measurement temperature.

The particulate fractions were measured on either 1 L water samples filtered onto ashed/acid washed 25 mm glass fibre filters (GF/F, 0.7 μm nominal pore size) for POC, PON and POP or 0.5 L samples filtered onto 0.8 μm or 0.2 μm 25 mm polycarbonate filters for bSi and PIC respectively. Organic carbon and nitrogen content was measured using a Costech ECS 4010 CHN elemental analyser, organic phosphorous was measured using the digestion method of Raimbault et al. (1999), bSi was measured using the method of Ragueneau and Treguer (1994), and PIC concentrations were measured using Inductively Coupled Plasma Atomic Mass Spectrometry (ICP-MS) (Green et al., 2003). Further details of sampling and analytical procedures can be found in Painter et al. (2016) with access to data via Painter (2017). In the following analysis we assume a basic premise that measured particulate pools represent biomass, a working assumption that is explored further in the discussion.

The mixed layer at each station was estimated using a density difference criteria of 0.03 kg m^{-3} relative to near surface values (de Boyer Montegut et al., 2004).

In the following, average nutrient and particulate pool concentrations and elemental stoichiometries for the mixed layer and for the water column beneath the mixed layer (the "benthic" layer) are presented. Technically this benthic layer definition includes intermediate and true benthic waters (those in contact with the seabed) but for simplicity the term benthic layer is used. Due to significant differences in water column depth between stations the depth of the benthic layer was limited to ~300 m off shelf to avoid introducing a deepwater bias into the calculations (i.e. at stations where the seabed was > 300 m deep the offshelf 'benthic' layer stretched from the base of the mixed layer to a maximum depth of 300 m). At four inner shelf stations (B1, C1, C2 and G1) the water column was fully mixed and no benthic layer could be identified. For these stations the mean mixed layer concentrations were replicated as a benthic layer estimate.

2.2. Historical observations

A supporting reanalysis of historical observations was also undertaken to provide a broader seasonal and annual context to place the cruise observations within. This incorporated analyses of satellite chlorophyll, inorganic and organic nutrients and particulate datasets.

2.2.1. Satellite observations of Chl-a

A time-series analysis of MODIS Aqua surface chlorophyll concentrations for the period 2002–2015 based on 8-day composite images (4 km resolution, reprocessing R2014) was undertaken to provide an overview of the phytoplankton seasonal cycle for a region of the shelf (56–58°N, 8–9°W) and for the adjacent ocean (56–58°N, 12–14°W). For each MODIS Aqua image all valid retrievals within the designated regions were averaged to provide a mean chlorophyll concentration at a single time point for the shelf and ocean time series respectively. Further details of the data processing are provided in the supplementary materials.

2.2.2. Inorganic nutrients

Inorganic nutrient data from the Land Ocean Interaction Study-Shelf

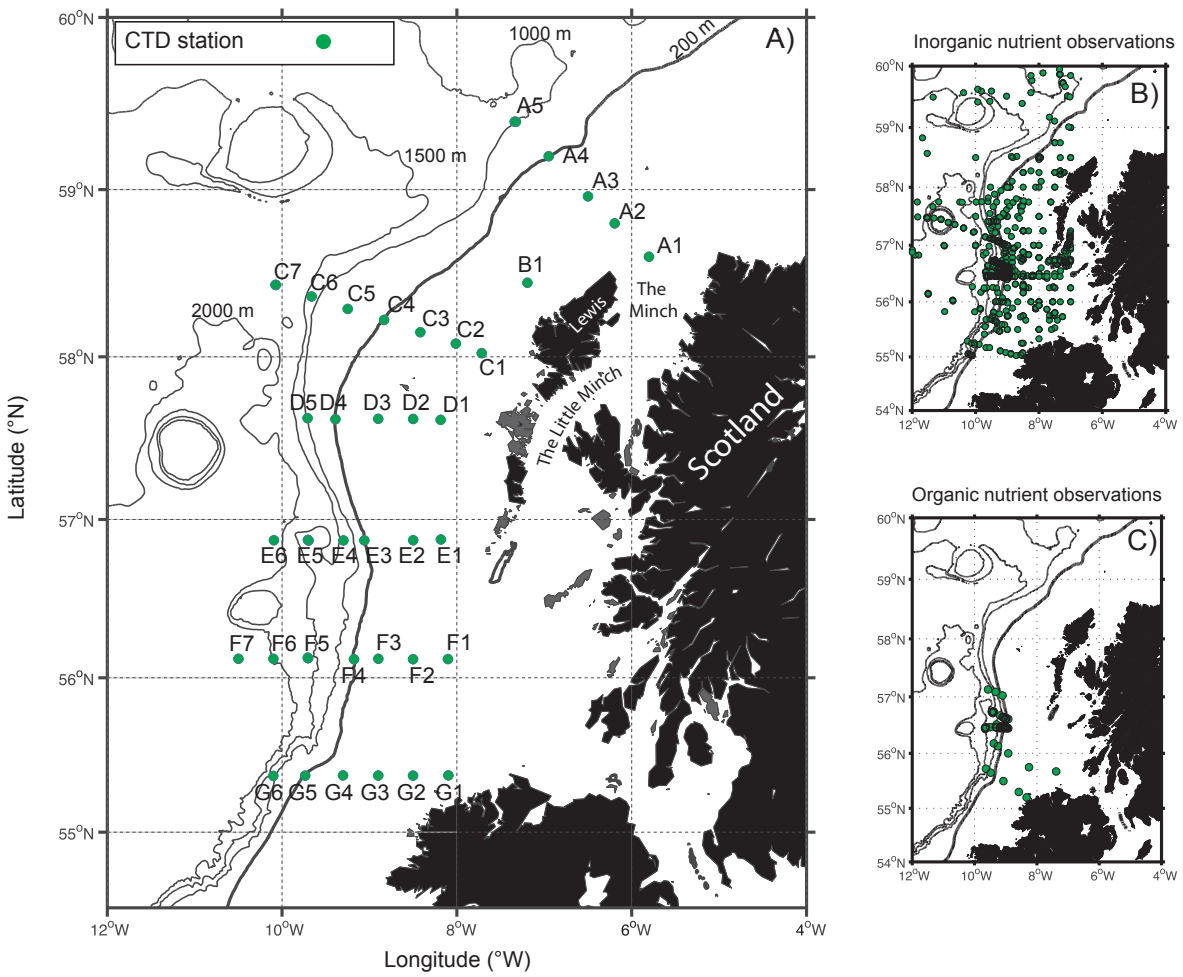

Fig. 1. Map of the Hebrides Shelf region showing (a) Station positions sampled during the October-November 2014 survey, (b) Distribution of historical (1960–2014) inorganic nutrient samples collated from the World Ocean Database (WOD) and Land Ocean Interaction Study-Shelf Edge Study (LOIS-SES) datasets, and (c) Distribution of dissolved organic nutrient samples collated from various sources (see text for details).

Edge Study (LOIS-SES; 1995–96 (Leeks and Jarvie, 1998; LOIS-SES Project Members, 1999)) and from the World Ocean Database (WOD; 1960–2014 (Boyer et al., 2013)) were collated and reanalysed. Nutrient observations from the upper 20 m of the water column and within 30 m of the seabed were used to construct monthly mean nutrient concentrations and nutrient stoichiometries for the mixed layer and benthic layer respectively, providing the seasonal context for the Hebrides Shelf region (55–60°N, 7–12°W; Fig. 1b). Use of a constant mixed layer depth and/or benthic layer thickness may simplify seasonal variability in both layers but the aim here was to provide a simple seasonal index for comparative purposes. Results are presented from the analysis of the combined dataset which consisted of 6573 individual observations of phosphate, silicate or nitrate from 808 unique locations across the shelf, shelf break and offshelf regions for the period 1960–2014 (Fig. 1b).

2.2.3. Organic nutrients

Organic nutrient observations for the Hebrides Shelf region were collated from the literature. Such observations are scarce for this region and strongly biased towards dissolved organic carbon (DOC) and nitrogen (DON) measurements, with few dissolved organic phosphorous (DOP) observations reported previously. Observations were collated from the LOIS-SES study (LOIS-SES Project Members, 1999), the OMEX study (OMEX Project Members, 1997) and from Moschonas et al. (2015). In total between 109 and 446 measurements of DOC, DON or DOP from 86 unique positions across the shelf, shelf break and offshelf regions were identified (Fig. 1c). In the majority of cases DON and DOP concentrations were calculated by difference between reported total dissolved nitrogen (TDN) or phosphorous (TDP) concentrations and concurrent measurements of inorganic NO_3^- (plus NO_2^-) and PO_4^{3-} pools reported in the original source publication/dataset. There was insufficient data to calculate monthly average concentrations for either the surface layer (upper 20 m) or the benthic layer (lower 30 m) for a full year thus only a seasonal analysis is presented.

2.2.4. Particulate datasets

Measurements of POC, PON and POP concentrations are also rare for this region. Consequently, a broader analysis of, and comparison to, coastal and oceanic particulate measurements collated and reported by Sterner et al. (2008) and Martiny et al. (2013,2014) was undertaken. These analyses focussed on comparisons of coastal and oceanic POC, PON and POP particulate concentrations and stoichiometric relationships to the 2014 cruise data to determine significant differences or notable agreements within the new observations reported here.

2.3. Spatial analysis

Both the new measurements from 2014 and the collated historical observations were analysed to obtain a mean regional picture of surface and benthic layers before being split into sub-regions (shelf, shelf break and ocean) and reanalysed to determine the presence and extent of intraregional variability in nutrient concentrations and stoichiometry, differences in timing of the seasonal cycle and region specific

characteristics. The datasets were split by water column depth denoting shelf (< 150 m), shelf break (150–280 m) and open ocean (> 280 m) sub-regions with depth ranges determined by approximate shelf break frontal positions. This separation of data resulted in a 6 box conceptual model of a coupled shelf-ocean system that allowed identification of differences in vertical gradients between layers and horizontal gradients between sub-regions with the aim of investigating the relevance of these for carbon export from the shelf to the ocean.

3. Results

3.1. Hebrides shelf

Surface chlorophyll concentrations by late October 2014 were low, around 0.4 ± 0.15 mg Chl-a m^{-3} (Fig. S1) placing the cruise in the post-autumn bloom period (Fig. S2). Mean chlorophyll concentrations for both shelf and offshelf regions were comparable to mid-winter concentrations observed in February (~0.4–0.5 mg Chl-a m^{-3}), and far lower than typically seen during the spring bloom in May/June (> 2 mg Chl-a m^{-3}) implying a weakly productive or non-productive system at the time of sampling (see supplementary material for further information on the phytoplankton annual cycle).

3.1.1. Inorganic nutrient pools

Mean mixed layer NO_3^- concentrations for autumn 2014 ranged from 2.02 to 6.40 μmol L^{-1} between stations with an overall mean (± s.d.) of 4.68 ± 1.06 μmol L^{-1} (Fig. 2a). A north–south gradient was evident with lower mean mixed layer concentrations towards the south (Fig. S3; see also Painter et al., 2016 for maps of horizontal nutrient distributions). Mean benthic layer NO_3^- concentrations ranged from 2.02 to 13.58 μmol L^{-1} with the lowest value representing station G1, where the water column was fully mixed, and the highest value representing station A4. The mean benthic layer NO_3^- concentration of 9.42 ± 3.56 μmol L^{-1} was ~2-fold higher than the mean mixed layer concentration. When grouped into sampled sub-region (i.e. shelf, shelf break and ocean) the mean mixed layer NO_3^- concentration gradually increased from the shelf (4.25 ± 1.0 μmol L^{-1}) to the ocean (5.18 ± 0.98 μmol L^{-1}) (Table 1). A similar but stronger gradient was also evident in the benthic layer with mean concentrations increasing from 7.15 ± 3.5 μmol L^{-1} on the shelf to 11.95 ± 1.02 μmol L^{-1} offshelf.

Mean mixed layer Si concentrations ranged from 0.47 to 2.37 μmol L^{-1}, with an overall mean of 1.49 ± 0.41 μmol L^{-1} (Fig. 2b). The shelf sub-regional mean concentration of 1.68 ± 0.34 μmol L^{-1} (Table 1) was significantly higher (*t*-test, $p < .01$) than the mean concentration at the shelf break or offshelf (1.28 ± 0.43 and 1.27 ± 0.37 μmol L^{-1} respectively). Si concentrations within the mixed layer therefore increased towards the coast. In the benthic layer mean Si concentrations ranged from 1.22 to 4.47 μmol L^{-1} with the lowest value found at station G3. Unusually, at this shelf station the mean Si concentration in the benthic layer (30–96 m depth range; 1.22 ± 0.09 μmol L^{-1}) was actually lower than the mean concentration in the mixed layer (0–21m; 1.32 ± 0.06 μmol L^{-1}). The mean benthic layer Si concentration of 3.16 ± 1.02 μmol L^{-1} was ~2-fold higher than the mixed layer. Despite the clear increase in mean mixed layer Si concentrations towards the coast the reverse was true within the benthic layer with the shelf mean concentration of 2.64 ± 1.07 μmol L^{-1} being ~30% lower than the oceanic sub-regional mean of 3.74 ± 0.61 μmol L^{-1} (Table 1).

Average PO_4^{3-} concentrations in the mixed layer ranged from 0.26 to 0.47 μmol L^{-1} with an overall mean concentration of 0.36 ± 0.05 μmol L^{-1} (Fig. 2c). No significant differences between shelf, shelf break and oceanic sub-regions could be identified due to negligible differences in the mean mixed layer PO_4^{3-} concentration between the three sub-regions (Table 1). PO_4^{3-} was thus the least variable of the three measured macronutrients within the surface mixed layer. In the benthic layer, mean PO_4^{3-} concentrations ranged from 0.26 to 0.87 μmol L^{-1} between stations with a cruise mean of 0.61 ± 0.18 μmol L^{-1}. Benthic layer PO_4^{3-} concentrations were thus generally less than 2-fold (69%) higher than the mixed layer concentration. The mean concentration for the shelf sub-region was 0.50 ± 0.18 μmol L^{-1} and was significantly lower (*t*-test, $p < .01$) than the corresponding mean ocean sub-regional concentration of 0.72 ± 0.07 μmol L^{-1} indicating that PO_4^{3-} concentrations increased towards the ocean.

Mean DIC concentrations within the surface mixed layer ranged from 2155.1 to 2177.1 μmol L^{-1} with a cruise mean of 2165.1 ± 5.02 μmol L^{-1} (Fig. 2d; equivalent to 2102.7–2123.9 μmol kg^{-1}, mean 2112.3 ± 4.78 μmol kg^{-1}). Concentration differences between stations within the mixed layer were ~1% and no significant differences could be identified between the three sub-regions (Table 1). In the benthic layer DIC concentrations were higher ranging from 2156.5 to 2223.8 μmol L^{-1} (equivalent to 2104.3–2169.5 μmol kg^{-1}) and were more variable (note that station G1 was fully mixed and hence presents with a relatively low DIC concentration). The mean benthic DIC concentration was 2192.4 ± 20.0 μmol L^{-1} (2138.9 ± 19.4 μmol kg^{-1}) and thus 27.3 μmol L^{-1} or ~1.3% higher than the mean mixed layer DIC concentration. Unlike the surface mixed layer significant differences in the mean benthic DIC concentration were identified between the three sub-regions (Table 1), with the shelf break (2209.3 ± 8.8 μmol L^{-1}) rather than the oceanic (2198.6 ± 7.7 μmol L^{-1}) sub-region having the highest mean DIC concentration.

3.1.1.1. Nutrient stoichiometry. DIC:NO_3^- within the mixed layer was higher than within the benthic layer at all stations except those where the water column was fully mixed (Fig. 3a). There was an approximately 3-fold variation in DIC:NO_3^- within the mixed layer between stations but a ~7-fold variation within the benthic layer mostly due to the southernmost Transect G. Mixed layer DIC:NO_3^- decreased towards the ocean (Table 1) and as a result the difference in DIC:NO_3^- between the shelf and the ocean was statistically significant but only at a reduced significance level (*t*-test, $p < .1$). Although the mean benthic layer DIC:NO_3^- (306.3 ± 191.4) was lower than that of the surface mixed layer (501.4 ± 157.5; Table 1) the contrast between the three sub-regions was greater within the benthic layer. The mean shelf ratio of 407.8 ± 222.7 was higher than found at the shelf break (185.4 ± 24.6) or oceanic (206.1 ± 40.0) sub-regions. Thus despite increased concentrations of DIC and NO_3^- in the benthic layer (Fig. 2), the seaward decrease in DIC:NO_3^- meant that shelf benthic waters were the most carbon rich waters (relative to NO_3^-) across the region (Table 1).

The same spatial patterns were also broadly present in DIC:PO_4^{3-} and DIC:Si (Fig. 3b, c), though with some notable exceptions. Both DIC:PO_4^{3-} and DIC:Si were higher in the surface mixed layer than within the benthic layer signifying a deficit of Si or PO_4^{3-} in surface waters compared to deeper waters (Table 1). However, whilst the station-to-station variability in DIC:PO_4^{3-} increased vertically from < 2-fold in the mixed layer to > 3-fold within the benthic layer the station-to-station variability in DIC:Si decreased vertically from > 5-fold in the mixed layer to ~4-fold in the benthic layer. Despite the vertical variability, and a weak seaward decrease in surface DIC:PO_4^{3-}, the mean DIC:PO_4^{3-} in the surface mixed layer was not significantly different between any of the three sub-regions (Table 1). Within the benthic layer a significant seaward decrease in DIC:PO_4^{3-} was evident between the shelf and the ocean (*t*-test, $p < .01$), however this gradient was non-linear and complicated by the lowest sub-regional mean DIC:PO_4^{3-} being found at the shelf break (Table 1). Nevertheless, the presence of a lateral gradient in benthic DIC:PO_4^{3-} and of higher DIC:PO_4^{3-} with depth across the region indicates that PO_4^{3-} was increasingly scarce in the benthic layer due to the increase of DIC with depth, a pattern consistent with that diagnosed from DIC:NO_3^- distributions.

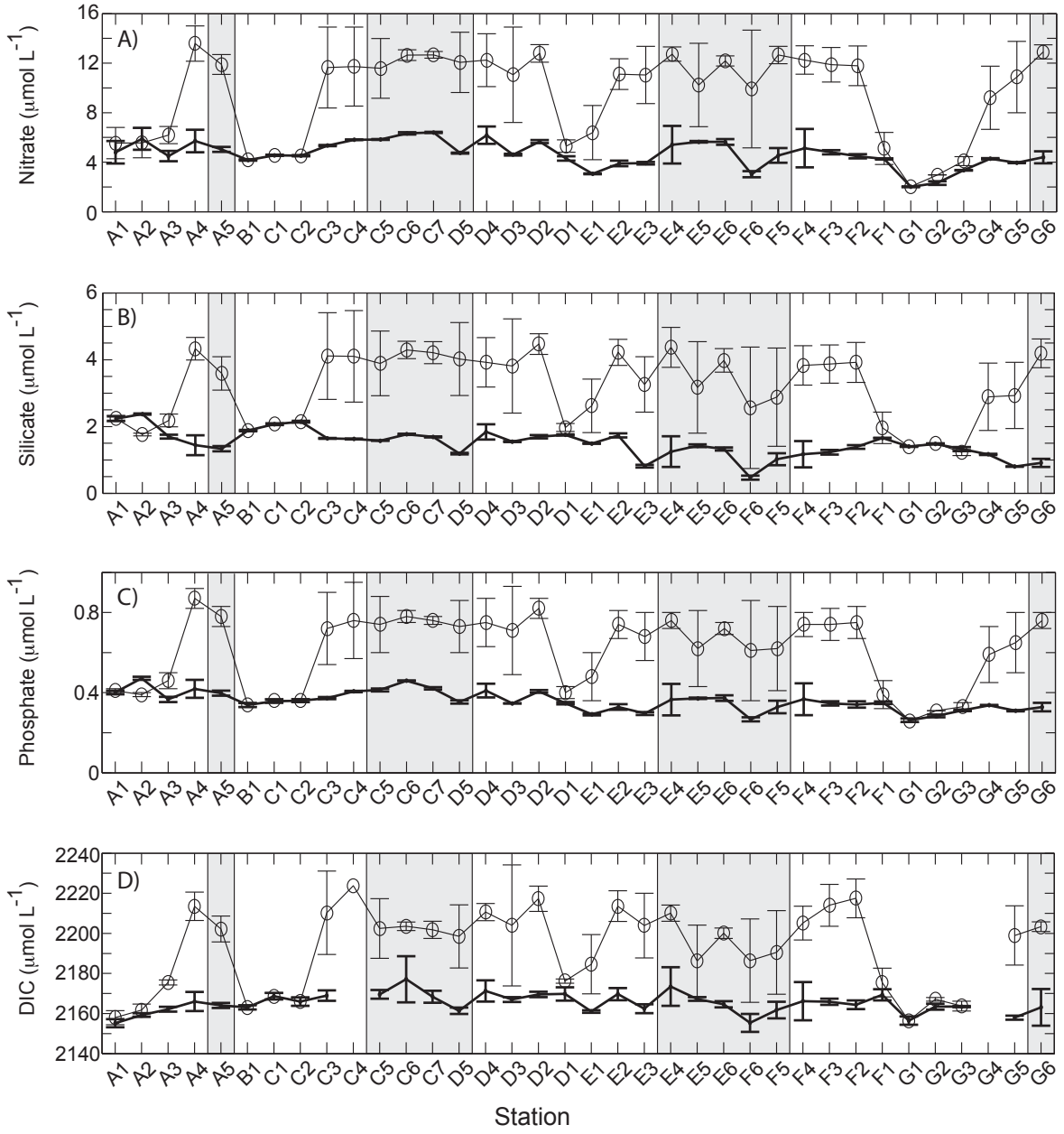

Fig. 2. Mean (± s.d.) nutrient concentrations as sampled in October-November 2014 averaged over the mixed layer (thick black line) and benthic layer (thin black line). Grey and white shading is used to indicate ocean and shelf subregions respectively.

Mean DIC:Si within the two layers revealed opposing seaward gradients. In the surface mixed layer DIC:Si was lowest on the shelf (1309 ± 236:1) and increased seawards with significant shelf-to-ocean differences being found (Table 1). In the benthic layer not only was DIC:Si ~50% lower than in the surface mixed layer but DIC:Si *decreased* from the shelf (992 ± 366:1) towards the shelf break and ocean (718 ± 273:1). These contrasting gradients suggest that the surface mixed layer was comparatively more Si rich relative to DIC on the shelf than offshore potentially signifying a terrestrial or riverine source of Si, but also that the benthic layer was increasingly Si rich in the seaward direction.

NO_3^-:PO_4^{3-} was lower within the surface mixed layer (mean 12.9 ± 1.7) than within the benthic layer (mean 14.8 ± 2.1) (Table 1). Generally, NO_3^-:PO_4^{3-} in the benthic layer was closer to the Redfield ratio of 16:1 (Redfield et al., 1963) while surface waters were depleted in NO_3^- relative to PO_4^{3-} (lower mean NO_3^-:PO_4^{3-}; Fig. 3d). Within the surface mixed layer NO_3^-:PO_4^{3-} increased seawards from a mean shelf value of 12.07 ± 1.74 to an oceanic value of 13.88 ± 1.18 indicating the potential for a stronger nitrogen deficit on shelf. In the lower layer NO_3^-:PO_4^{3-} also increased seawards from a shelf mean value of 13.5 ± 2.2 to an oceanic value of 16.3 ± 0.6. In both layers the mean shelf and mean oceanic ratios were significantly different to one another (Table 1). Collectively these results indicate that shelf waters were generally depleted in NO_3^- relative to PO_4^{3-}.

The mean NO_3^-:Si in the surface mixed layer was 3.37 ± 1.1 though it varied over 4-fold between stations and was above the value of 1:1 often assumed for balanced diatom growth (Brzezinski, 1985; Fig. 3e). Surface waters were therefore Si poor relative to NO_3^-. Note however that inter-species variability in optimal cellular N:Si urges caution when interpreting NO_3^-:Si for indications of NO_3^- or Si limitation (Tett et al., 2003; Gilpin et al., 2004). A clear seaward increase in NO_3^-:Si was evident between sub-regions with mean ratios of 2.58 ± 0.67 on the shelf, 4.19 ± 0.65 at the shelf break and 4.3 ± 0.82 offshore. Only differences between the shelf and the ocean

Table 1
Mean (± s.d.) mixed and benthic layer nutrient concentrations and selected mean nutrient ratios in those layers. Differences in the mean concentrations between different sampled regions (shelf, shelf break and ocean) were assessed via a student's *T*-test and statistical p-values are presented to three levels of significance ($p < .1$, $p < .05$, $p < .01$); ns = not significant.

Layer	Region	NO_3 (μmol L^{-1})	Si (μmol L^{-1})	PO_4 (μmol L^{-1})	DIC (μmol L^{-1})	$DIC:NO_3$	$DIC:PO_4$	DIC:Si	NO_3:PO_4	NO_3:Si	Si: PO_4
Mixed layer	Shelf	4.25 ± 1.0	1.68 ± 0.34	0.35 ± 0.05	2164.62 ± 4.55	552.1 ± 184.0	6331.6 ± 856.6	1309.3 ± 235.9	12.1 ± 1.7	2.6 ± 0.7	4.8 ± 0.7
	Shelf break	5.12 ± 0.98	1.28 ± 0.43	0.37 ± 0.05	2164.75 ± 4.96	457.9 ± 88.7	6208.7 ± 922.8	2024.5 ± 663	13.8 ± 0.8	4.2 ± 0.7	3.4 ± 0.7
	Ocean	5.18 ± 0.98	1.27 ± 0.37	0.37 ± 0.05	2165.99 ± 6.06	438.2 ± 105.6	5978.9 ± 916.1	1961.5 ± 958.5	13.9 ± 1.2	4.3 ± 0.8	3.3 ± 0.6
	All	4.68 ± 1.06	1.49 ± 0.41	0.36 ± 0.05	2165.08 ± 5.02	501.4 ± 157.5	6199.4 ± 872.5	1625.5 ± 690.4	12.9 ± 1.7	3.4 ± 1.1	4.1 ± 1.0
p-value	Ocean vs shelf	$p < .05$	$p < .01$	ns	ns	$p < .1$	ns	$p < .01$	$p < .01$	$p < .01$	$p < .01$
	Ocean vs break	ns	ns	ns	ns	ns	ns	ns	ns	ns	ns
	Shelf vs break	$p < .1$	$p < .05$	ns	ns	ns	ns	$p < .01$	$p < .05$	$p < .01$	$p < .01$
Benthic layer	Shelf	7.15 ± 3.5	2.64 ± 1.07	0.50 ± 0.18	2182.93 ± 22.9	342.7 ± 157.8	4550.1 ± 1431.1	935.6 ± 382.5	14.1 ± 1.8	2.8 ± 0.4	5.1 ± 0.5
	Shelf break	11.95 ± 0.99	3.73 ± 0.53	0.74 ± 0.07	2209.31 ± 8.76	185.4 ± 24.6	2960.1 ± 418.2	619.5 ± 165.0	16.1 ± 0.5	3.3 ± 0.3	4.9 ± 0.4
	Ocean	11.95 ± 1.02	3.74 ± 0.61	0.72 ± 0.07	2198.64 ± 7.66	205.9 ± 40.1	3294.3 ± 546.7	716.8 ± 273.6	16.3 ± 0.6	3.3 ± 0.5	5.1 ± 0.6
	All	9.42 ± 3.56	3.16 ± 1.02	0.61 ± 0.18	2192.39 ± 20.03	263.8 ± 129.6	3796.8 ± 1230.3	796.8 ± 332.4	15.2 ± 1.6	3.1 ± 0.5	5.1 ± 0.5
p-value	Ocean vs shelf	$p < .01$	$p < .01$	$p < .01$	$p < .05$	$p < .01$	$p < .05$	Ns	$p < .01$	$p < .01$	ns
	Ocean vs break	ns	ns	ns	$p < .05$	ns	ns	ns	ns	ns	ns
	Shelf vs break	$p < .01$	$p < .05$	$p < .01$	$p < .05$	$p < .05$	$p < .05$	$p < .1$	$p < .05$	$p < .05$	ns
Layer difference	Shelf	3.67 ± 3.01	1.22 ± 1.23	0.2 ± 0.18	23.55 ± 20.56						
	Shelf break	6.83 ± 0.74	2.45 ± 0.31	0.37 ± 0.04	41.66 ± 3.44						
	Ocean	6.77 ± 1.09	2.47 ± 0.49	0.34 ± 0.05	32.65 ± 6.14						
	All	5.33 ± 2.66	1.88 ± 1.08	0.28 ± 0.15	29.91 ± 15.82						

or the shelf and the shelf break were significantly different (Table 1) suggesting that the ocean and shelf break were chemically similar but distinct to the shelf. The mean NO_3^-:Si within the benthic layer was 2.95 ± 0.56 and ~13% lower than that of the surface mixed layer but at many stations there was very little difference between the two layers. Nevertheless, a seaward increase in the benthic NO_3^-:Si ratio was evident increasing from 2.64 ± 0.49 on the shelf to 3.29 ± 0.47 in the ocean. The shelf to ocean increase was significant (Table 1). NO_3^-:Si was greater than 1:1 everywhere indicating widespread silicate deficiency, perhaps unsurprising given the autumn sampling dates.

The mean $Si:PO_4^{3-}$ ratio was lower in the surface mixed layer (4.13 ± 1.01) than in the benthic layer (5.12 ± 0.53) (Fig. 3f). Within surface waters there was a significant seaward decrease in $Si:PO_4^{3-}$ from a shelf mean value of 4.82 ± 0.72 to a mean oceanic value of 3.34 ± 0.64 (Table 1). In the benthic layer there was no significant difference between shelf, shelf break or oceanic sub-regions with mean ratios ranging from 4.94 ± 0.36 to 5.18 ± 0.54. Though based predominately on diatom requirements (Brzezinski, 1985), if a typical $Si:PO_4^{3-}$ ratio of 15:1 is assumed appropriate for balanced growth the mean values obtained in both layers were well below this expectation suggesting severe Si deficiency in the nutrient pools. This is also not surprising given that observations were made late in the year, long after the spring bloom, the summer productive period and a modest autumn bloom (Fig. S2), and there was unlikely to have been significant recharging of Si concentrations as the water column was still stratified.

3.1.2. Particulate pools

Layer average concentrations of bSi, POC, PON, POP and PIC are shown in Fig. 4. The mean mixed layer bSi concentration (reported as Si not opal) was 0.31 ± 0.08 μmol Si L^{-1} and there was no significant difference in the mean concentration for shelf, shelf break or oceanic sub-regions (Table 2). At some stations however (e.g. stations C3, C7) there was significant vertical variability within the mixed layer but these were exceptions rather than the rule. Concentrations of bSi within the benthic layer were not that dissimilar to the surface layer with a mean concentration of 0.29 ± 0.06 μmol Si L^{-1} (Table 2). Variability in bSi concentrations within the benthic layer was slight but there was nevertheless a significant difference between the shelf mean concentration of 0.32 ± 0.07 μmol Si L^{-1} and the mean oceanic concentration of 0.26 ± 0.05 μmol Si L^{-1} suggesting a seaward decrease in bSi concentrations. This gradient could reflect the resuspension of bSi from shelf sediments.

The concentration of POC in the surface mixed layer averaged 6.5 ± 1.3 μmol C L^{-1} (Fig. 4b) and concentrations were broadly similar between the shelf, shelf break and ocean sub-regions ranging from 5.7 to 6.7 μmol C L^{-1} with the lowest mean concentration measured at the shelf break (Table 2). Mean POC concentrations in the benthic layer were lower with a mean concentration of 5.89 ± 2.37 μmol C L^{-1}. A seaward decrease from a mean shelf concentration of 6.74 ± 2.88 μmol C L^{-1} to a shelf break concentration of 5.9 ± 1.87 μmol C L^{-1} to an oceanic concentration of 4.73 ± 1.22 μmol C L^{-1} was evident with the shelf to ocean difference proving to be significant ($p < .05$; Table 2).

The mean PON concentration in the surface mixed layer was 0.76 ± 0.16 μmol N L^{-1} with insignificant differences between shelf, shelf break and oceanic sub-regions (Table 2). PON concentrations were ~25% lower in the benthic layer averaging 0.57 ± 0.23 μmol N L^{-1} but varied almost 2-fold along the cross shelf gradient from a maximum of 0.69 ± 0.22 μmol N L^{-1} on the shelf to a minimum of 0.37 ± 0.11 μmol N L^{-1} offshelf. The largest vertical differences in PON concentration, potentially signifying the strongest remineralization rates, were found at deeper stations (Fig. 4c).

At individual stations POP concentrations were generally higher in the surface mixed layer (range 0.03–0.1 μmol P L^{-1}) than within the benthic layer (range 0.01–0.07 μmol P L^{-1}; Fig. 4d). Consequently, the

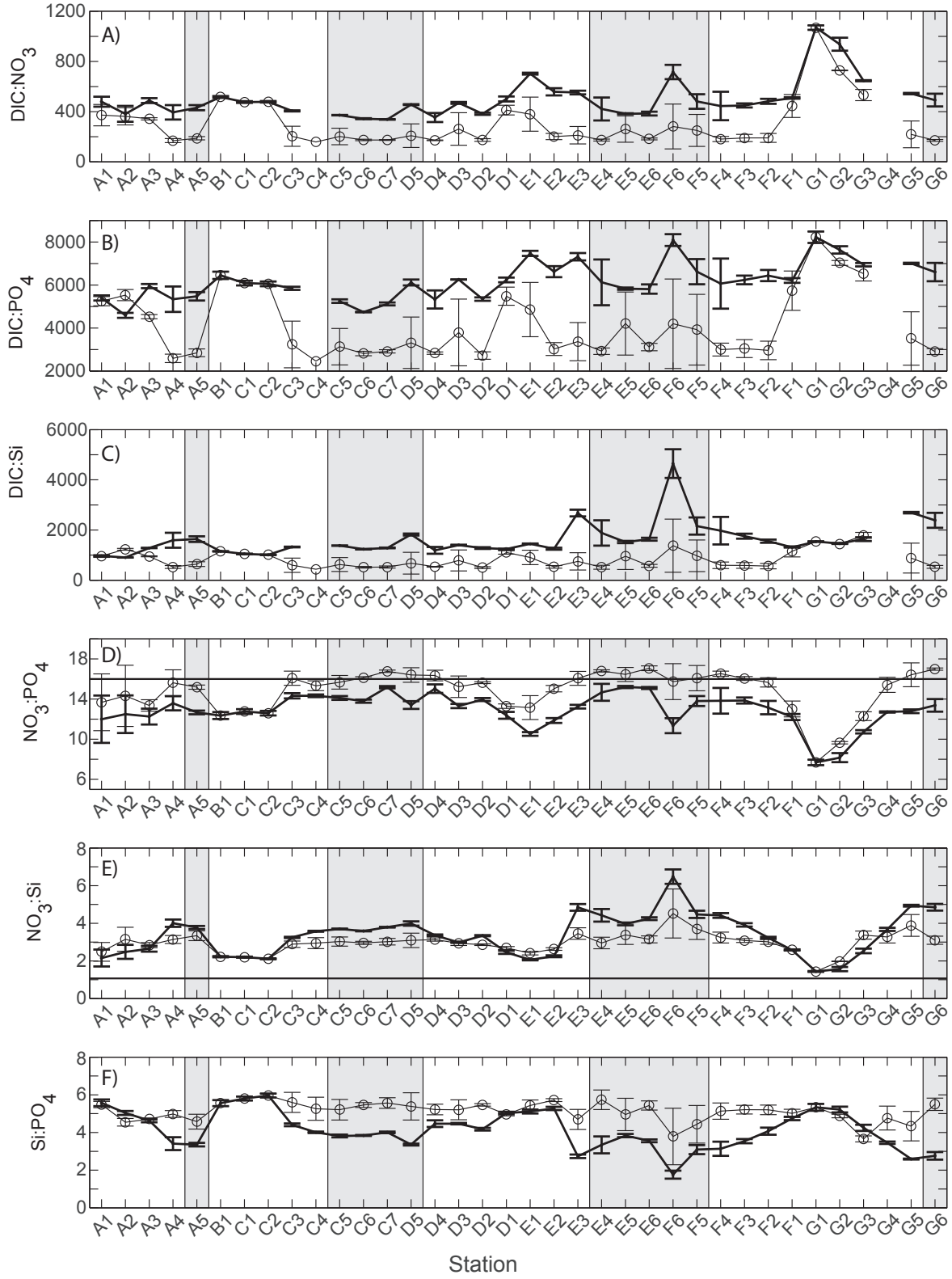

Fig. 3. Selected nutrient stoichiometries for October-November 2014 averaged (± s.d.) over the mixed layer (thick black line) and benthic layer (thin black line). Grey and white shading is used to indicate ocean and shelf subregions respectively. Horizontal black lines denote Redfield stoichiometric ratios based on the standard stoichiometric formula of 106C:15Si:16N:1P.

mean surface layer POP concentration of 0.05 ± 0.01 μmol P L^{-1} was significantly higher than that of the benthic layer (0.03 ± 0.01 μmol P L^{-1}; $p < .001$; Table 2). Within each layer however different distributions were evident with negligible and non-significant differences in mean POP concentrations horizontally between the three sampled sub-regions in the surface mixed layer and small but significant differences between the shelf and the shelf break or ocean sub-regions in the benthic layer (Table 2).

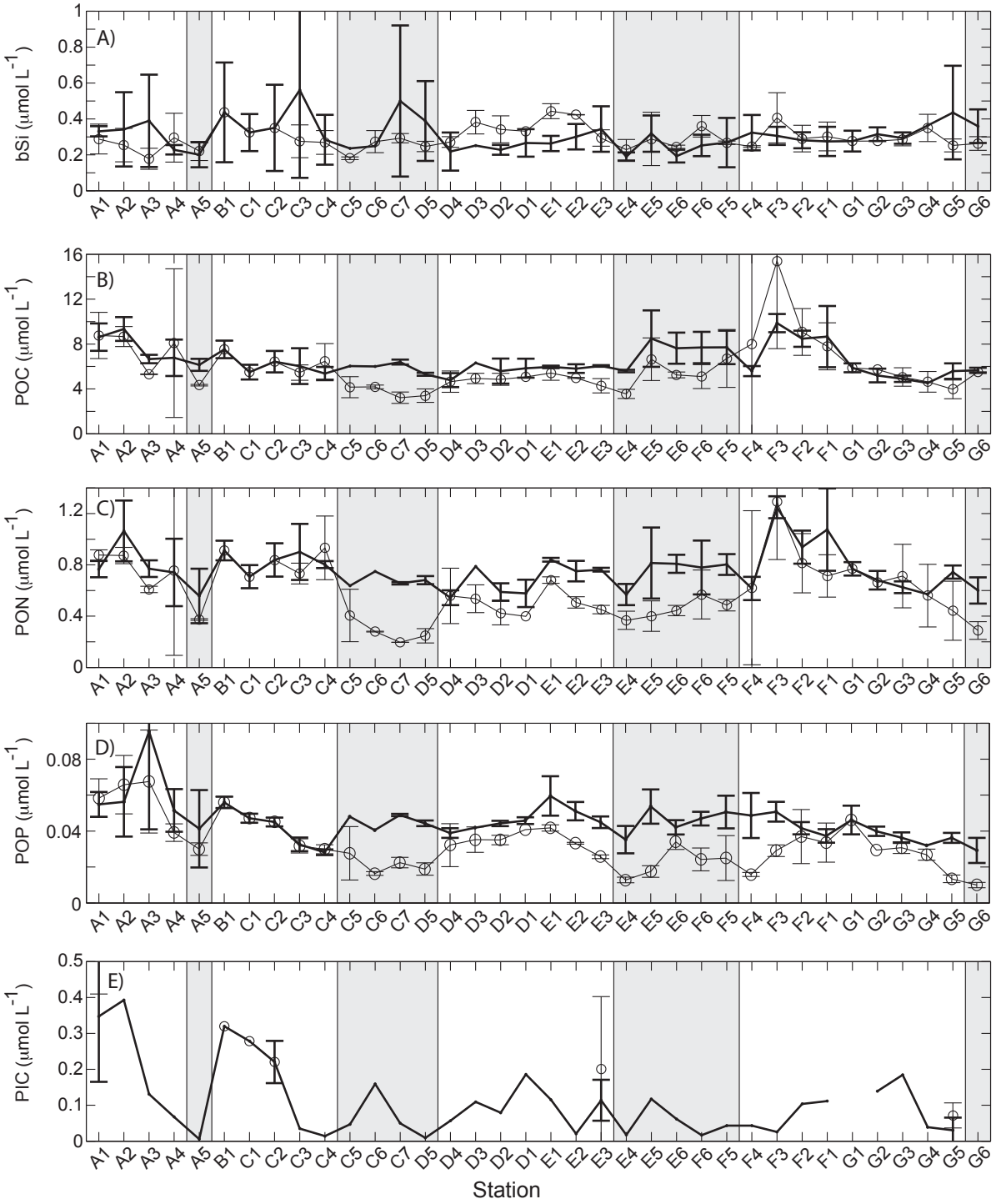

Fig. 4. Mean (± s.d.) particulate concentrations for October-November 2014 for the mixed layer (thick black line) and benthic layer (thin black line). Grey and white shading is used to indicate ocean and shelf subregions respectively. Note that PIC samples were primarily collected at the sea surface only (< 10 m) with reduced vertical sampling through the mixed and benthic layers compared to the other particulate pools.

Surface PIC concentrations ranged from 0.01 to 0.39 μmol L^{-1} with a mean of 0.11 ± 0.1 μmol L^{-1} and concentrations were highest at the most inshore stations along transect A (Fig. 4e). Benthic PIC concentrations were poorly constrained but ranged from 0.07 to 0.52 μmol L^{-1}.

3.1.2.1. Particulate stoichiometry. Stoichiometric ratios within the particulate pools are shown in Fig. 5, with mean values for the two layers presented in Table 2. The POC:PON ratio was above the Redfield C:N ratio of 6.6:1 at all stations and in both layers indicating the widespread presence of carbon rich particulate matter (Fig. 5a). Within the surface mixed layer the mean POC:PON ratio was 8.7 ± 1.3 (Table 2), but varied from a shelf mean of 8.3 ± 1.1 to an oceanic mean of 9.8 ± 1.2. The shelf and shelf break mean POC:PON ratios were significantly lower (*t*-test, $p < .01$, $p < .05$ respectively) than the mean oceanic POC:PON (Table 2). Variability within the surface mixed layer was relatively muted with the POC:PON varying ~2-fold from 6.7 to 12.2. In the benthic layer POC:PON was both more variable

Table 2
Mean (± s.d.) mixed layer and benthic layer particulate concentrations and selected mean elemental ratios in those layers. Differences in the mean particulate concentrations and mean elemental ratios between different sampled regions (shelf, shelf break and ocean) were assessed via a student's *t*-test and statistical p-values are presented to three levels of significance ($p < .1$, $p < .05$, $p < .01$); ns = not significant.

Layer	Region	bSi (μmol L^{-1})	POC (μmol L^{-1})	PON (μmol L^{-1})	POP (μmol L^{-1})	PIC (μmol L^{-1})	POC:PON	POC:POP	PON:POP	bSi:POP
Mixed layer	Shelf	0.32 ± 0.08	6.69 ± 1.58	0.81 ± 0.18	0.05 ± 0.01	0.16 ± 0.11	8.3 ± 1.11	147.7 ± 37	18.1 ± 5	7.4 ± 3.05
	Shelf break	0.31 ± 0.08	5.69 ± 0.67	0.7 ± 0.1	0.04 ± 0.01	0.05 ± 0.03	8.26 ± 1.07	142.4 ± 26.9	17.9 ± 5.9	7.86 ± 2.9
	Ocean	0.29 ± 0.1	6.6 ± 1.07	0.7 ± 0.1	0.04 ± 0.01	0.05 ± 0.05	9.75 ± 1.21	157.2 ± 25.5	16.4 ± 2.4	6.83 ± 2.58
	All	0.31 ± 0.08	6.5 ± 1.34	0.76 ± 0.16	0.05 ± 0.01	0.11 ± 0.1	8.74 ± 1.29	149.7 ± 32	17.5 ± 4.5	7.3 ± 2.82
p-value	Ocean vs shelf	ns	ns	$p < .1$	ns	0.01	$p < .01$	ns	ns	ns
	Ocean vs break	ns	$p < .1$	ns	ns	ns	$p < .05$	ns	ns	ns
	Shelf vs break	ns	ns	ns	ns	$p < .05$	ns	ns	ns	ns
Benthic layer	Shelf	0.32 ± 0.07	6.74 ± 2.88	0.69 ± 0.22	0.04 ± 0.01	0.52 ± 0	9.8 ± 1.67	187.04 ± 102.51	19.1 ± 8.4	9.2 ± 3.24
	Shelf break	0.27 ± 0.02	5.9 ± 1.87	0.63 ± 0.19	0.03 ± 0.01	0.14 ± 0.09	9.75 ± 1.91	259.97 ± 141.73	26.32 ± 9.82	11.93 ± 4.43
	Ocean	0.26 ± 0.05	4.73 ± 1.22	0.37 ± 0.11	0.02 ± 0.01	–	13.67 ± 3.12	251.58 ± 125.17	18.81 ± 7.02	14.27 ± 5.88
	All	0.29 ± 0.06	5.89 ± 2.37	0.57 ± 0.23	0.03 ± 0.01	–	11.12 ± 2.91	222.9 ± 119.25	20.36 ± 8.47	11.45 ± 4.94
p-value	Ocean vs shelf	$p < .05$	$p < .05$	$p < .01$	$p < .01$	–	$p < .01$	ns	ns	$p < .01$
	Ocean vs break	ns	ns	$p < .01$	ns	–	$p < .05$	ns	$p < .1$	ns
	Shelf vs break	ns	ns	ns	$p < .05$	–	ns	ns	ns	ns

between stations, ranging almost 3-fold from 7 to 19.7, and generally higher with a mean of 11.1 ± 2.9. On the shelf the mean benthic POC:PON of 9.8 ± 1.7 was significantly higher than measured in the surface mixed layer, but also significantly lower than measured offshelf, where the mean POC:PON ratio was 13.7 ± 3.1 (Table 2).

Mixed layer POC:POP varied almost 3-fold from 84:1 to 230:1 (mean 150 ± 32:1) thus POC:POP was generally elevated compared to the Redfield ratio. A weak cross shelf gradient was present with shelf POC:POP (148 ± 37:1) being lower than offshore (157 ± 26) (Table 2). In the benthic layer POC:POP was higher (Fig. 5b) varying from 86:1 to 560:1 denoting C rich/P poor material at depth. The mean oceanic POC:POP was 252 ± 125:1 but was not significantly higher than measured on the shelf (187 ± 103:1) due to the large variability in both sub-regions.

Mixed layer PON:POP ranged from 10:1 to 29:1 with a mean of 18 ± 5:1 that was slightly elevated above the Redfield ratio (Fig. 5c). There was limited variation between shelf (18.1 ± 5), shelf break (17.9 ± 5.9) and ocean (16.4 ± 2.4) sub-regions (Table 2) but the mean ratios nevertheless suggested the presence of a weak shelf to ocean gradient. In the benthic layer the mean PON:POP was higher (20.4 ± 8.5:1) and more variable ranging from 8.8:1 to 43.9:1. Despite broad station-to-station variability the mean benthic layer PON:POP of the shelf and ocean sub-regions were only slightly elevated compared to the Redfield ratio. The mean PON:POP ratio at shelf break stations (26.3 ± 9.8) was significantly higher ($p < .1$) than the oceanic value.

bSi:POP was similar between the two layers and generally less than the typical ratio assumed for diatoms of 15:1 (Brzezinski, 1985) (Fig. 5d). Mixed layer bSi:POP decreased towards the ocean from a shelf mean of 7.4 ± 3.1, via an increased shelf break mean of 7.86 ± 2.9 to an oceanic mean of 6.8 ± 2.6 (Table 2). Meanwhile benthic layer bSi:POP increased towards the ocean with a mean shelf value of 9.2 ± 3.2, shelfbreak value of 11.9 ± 4.4 and oceanic value of 14.3 ± 5.9. Differences between the shelf and ocean were significant (*t*-test $p < .05$; Table 2) but only at oceanic stations were the vertical differences between the two layers significantly different.

Overall, only minor differences were evident in the mean particulate stoichiometry between the surface waters of each sub-region. Consequently, the mean particulate stoichiometry could be approximated as 150C:7Si:18N:1P (Table 2). In the benthic waters the mean particulate stoichiometry was 223C:11Si:20N:1P, but was also more variable between sub-regions, thus the mean value may be indicative only (Table 2).

3.2. Relationship between particulate and environmental stoichiometry

The C:N of the particulate pool (i.e. POC:PON) was consistently and significantly lower than that of the environment (i.e. DIC:NO_3) in all sampled sub-regions resulting in a strong deviation away from the 1-to-1 line (Fig. 6a). Consequently the high environmental C:N, which indicated a C rich system, cannot be considered as having a direct influence on the lower equilibrium C:N of algal biomass. In contrast there was a much closer agreement between PON:POP and NO_3^-:PO_4^{3-} suggesting that the two were more strongly linked (Fig. 6b). There was however considerably more scatter in PON:POP than in NO_3^-:PO_4^{3-} indicating that the environmental NO_3^-:PO_4^{3-} was not an absolute regulator of algal biomass N:P. PON:POP was generally higher (N rich) than NO_3^-:PO_4^{3-} leading to a movement upward and away from the 1-to-1 line. This indicates that where deviations from a strict 1-to-1 relationship occurred the biomass was more likely to be N rich (and thus P poor) compared to the environment. It has been suggested that slow growing phytoplankton species typically found in surface waters after the spring bloom may be more susceptible to N rather than P limitation (Elrifi and Turpin, 1985; Hillebrand et al., 2013). The PON:POP data generally supports this suggestion because not only was the NO_3^-:PO_4^{3-} generally < 16:1 (i.e. P rich relative to Redfield; Table 1) but the particulate PON:POP was generally > 16:1 suggesting that the

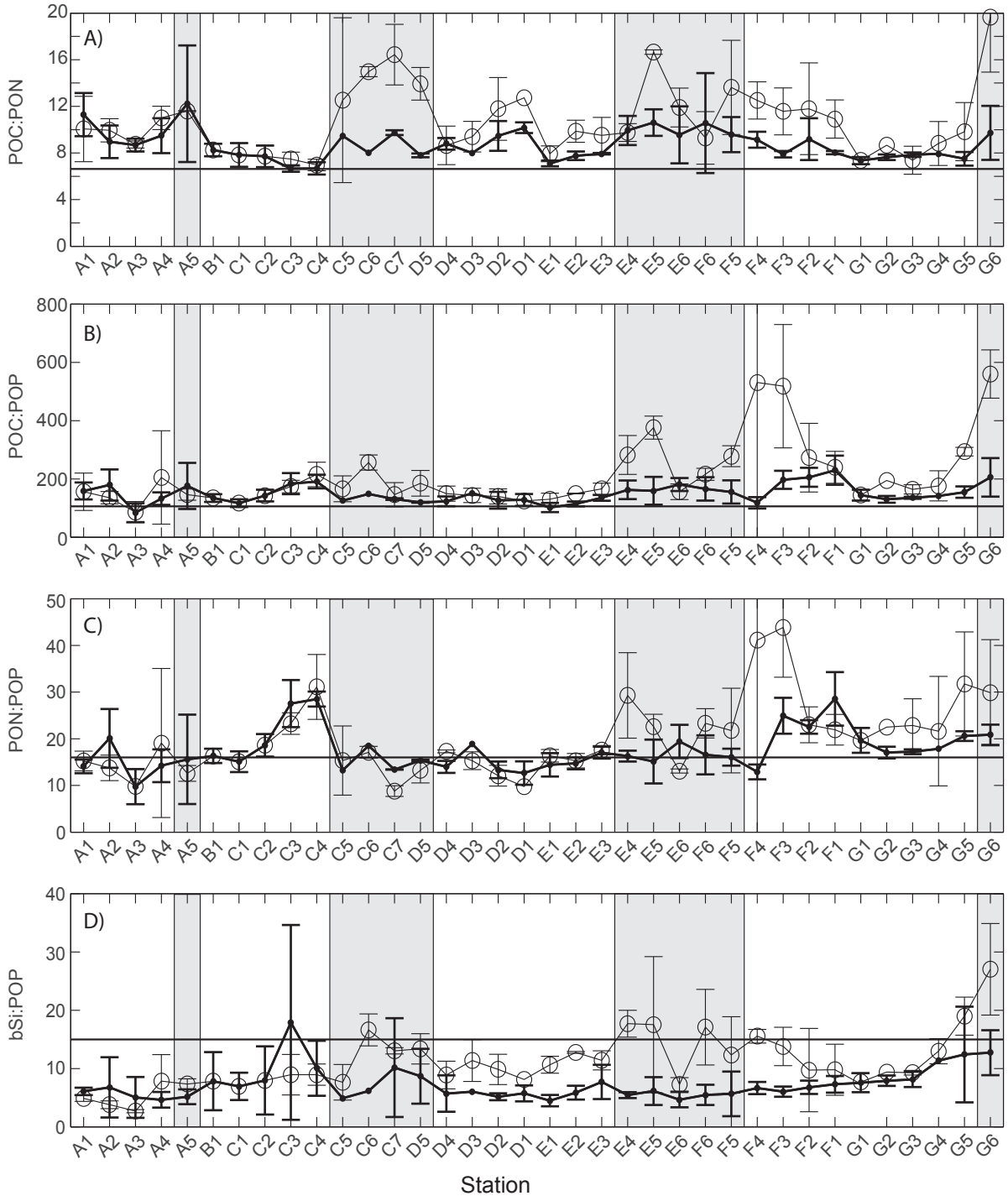

Fig. 5. Selected particulate stoichiometries for October-November 2014 averaged (± s.d.) over the mixed layer (thick black line) and benthic layer (thin black line). Grey and white shading is used to indicate ocean and shelf subregions. Horizontal black lines denote Redfield stoichiometric ratios based on the standard stoichiometric formula of 106C:15Si:16N:1P.

biomass was preferentially N rich relative to the environmental nutrient pool (Table 2).

Inorganic C:P ratios (i.e. DIC:PO_4^{3-}) were distinctly higher than the corresponding biomass C:P (i.e. POC:POP) again indicating that the environmental supply of C was not an immediate constraint on the C:P ratio of the biomass (Fig. 6c). N:Si was also examined (Fig. 6d), which revealed a strong similarity between nutrient and particulate pools. The data clustered around the 1-to-1 line with 47% of biomass data points having a higher N:Si (i.e N rich) than the environment, whilst 53% of data points had a lower N:Si. The relationship between environmental N:Si and biomass N:Si was surprisingly strong despite Si being utilised early in the year which may indicate the presence of longer-term Si control on algal biomass. Indeed, seasonal diatom distributions for this region reveal residual diatom communities on the shelf after the spring bloom thought due to higher ambient silicate concentrations and favourable N:Si conditions (Fehling et al., 2012; Siemering et al., 2016).

A similar analysis was undertaken for the benthic layer (Fig. 6). The results mirrored those for the mixed layer indicating that no significant change in the relationship between the particulate pool and the nutrient pool occurred with depth. Nevertheless subtle shifts in the relationships were evident. These were most clearly visible in the N:P and N:Si relationships (Fig. 6b, d) which both revealed larger changes to the

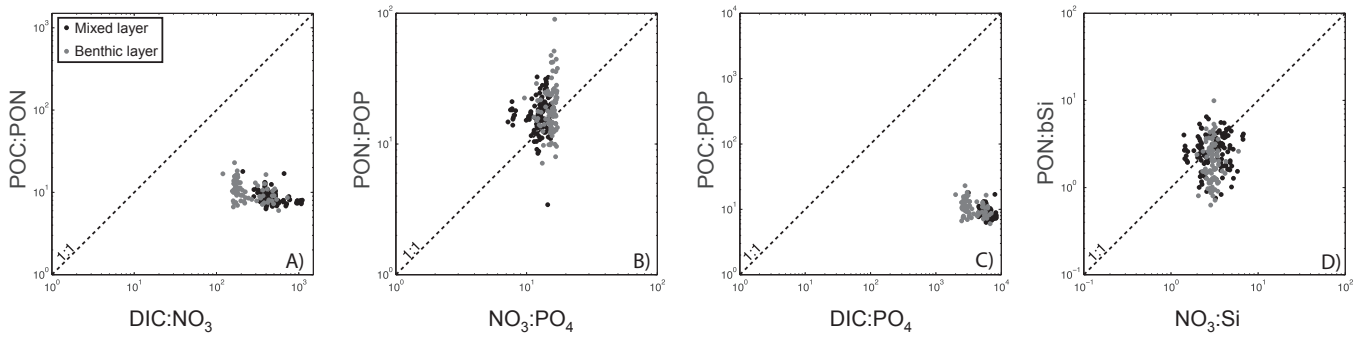

Fig. 6. Relationships between inorganic nutrient (substrate) stoichiometry and particulate (biomass) stoichiometry for the mixed layer (black dots) and benthic layers (grey dots) based on samples collected in October-November 2014.

nutrient pool stoichiometry rather than to the particulate pool stoichiometry of the benthic layer.

To better understand the stoichiometry of the particulate pool and how it changed with depth between the surface and benthic layers ratio-ratio plots were used to clarify stoichiometric shifts due largely to microbial processes (Fig. 7a, b). In the surface mixed layer there was no clear sub-regional distinction in mean mixed layer PON:POP or bSi:POP. All stations, except station C3, indicated particulate material with low Si content relative to P (bSi:POP < 1 5) or to N (bSi:PON < 1). At station C3 the bSi:POP was elevated but the reason was not clear. More stations had PON:POP > 16:1 (21 stations) than < 16:1 (15 stations). In the benthic layer there were indications of

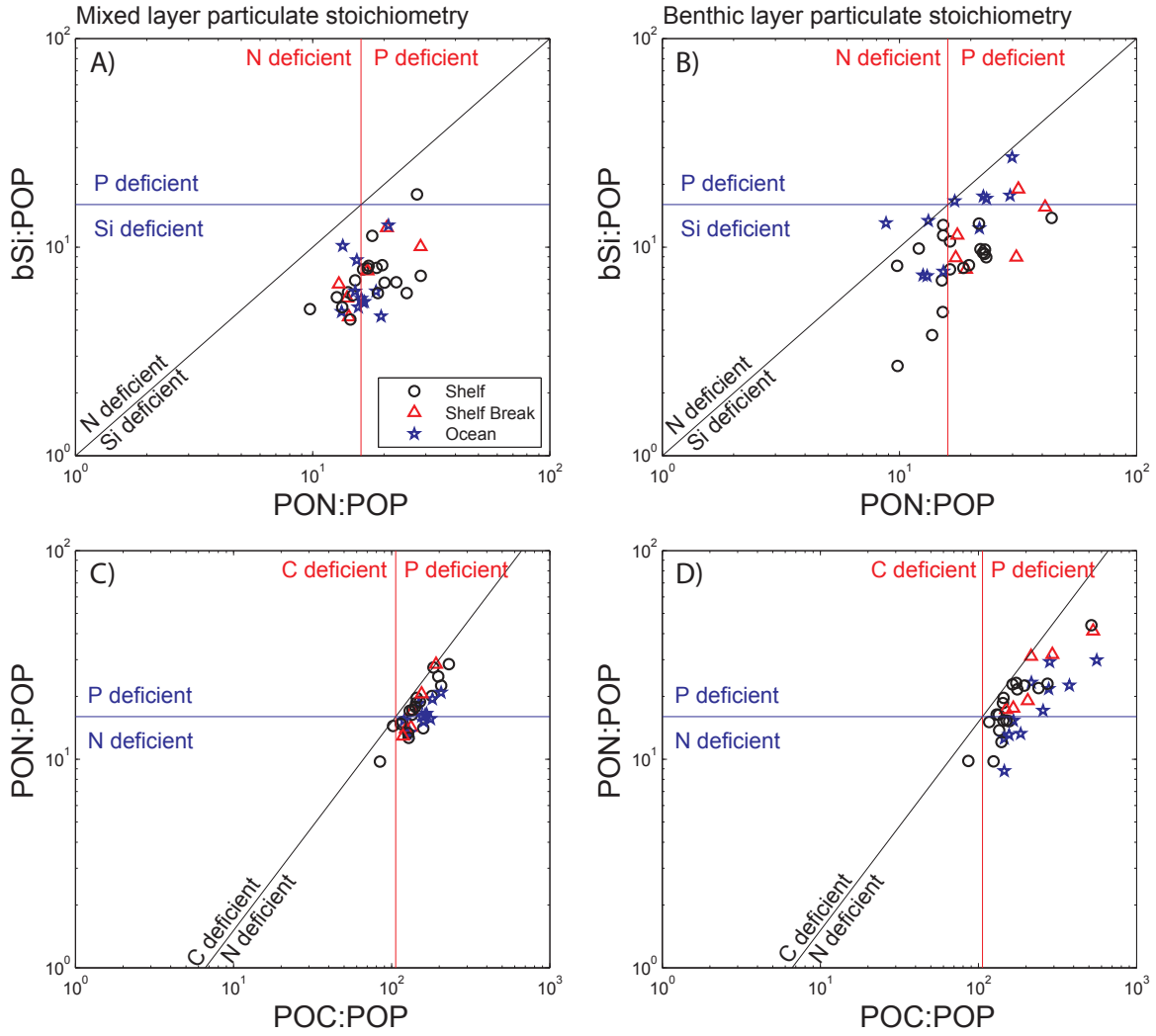

Fig. 7. Particulate ratio-ratio plots for the mixed layer (left hand column) and benthic layer (right hand column) of the shelf, shelf break and ocean subregions sampled in October-November 2014. The vertical red lines, horizontal blue lines and diagonal black lines represent Redfield stoichiometric ratios based on the standard stoichiometric formula of 106C:15Si:16N:1P. There is no indication of significant sub-regional variability within the mixed layer as all three subregions display a similar character but note the increased scatter in the data within the benthic layer and the subregional divergence between the shelf and ocean stations with oceanic particles tending towards a higher bSi:POP than particles on the shelf, and higher POC:PON than found on the shelf. (For interpretation of the references to colour in this figure legend, the reader is referred to the web version of this article.)

sub-regional differences but also of greater spatial variability. For example, whilst all shelf break stations shifted towards higher PON:POP (i.e. P loss), all ocean stations shifted towards higher bSi:POP (P loss), and all shelf stations shifted towards lower PON:POP (N loss), there was also greatly increased scatter such that no single region could be unambiguously distinguished.

An alternative plot focussed on the carbon content of the particulate pool (Fig. 7c, d) also revealed important stoichiometric shifts with depth. In the surface mixed layer the measurements were tightly clustered parallel to a C:N of 6.6 and generally revealed high POC:POP. In the benthic layer there was a clear shift towards higher POC:POP but with broad retention of a fixed C:N. Oceanic particulate material underwent the largest stoichiometric shift which may indicate stronger recycling, or more precisely P scavenging, in the oceanic water column than on the shelf. Shelf and shelf break stations underwent small increases in POC:POP but shelf stations typically also saw reductions in PON:POP which shelf break stations did not.

3.3. Annual context from historical observations

3.3.1. Inorganic nutrients

Mean monthly PO_4^{3-} concentrations ranged from 0.56 μmol L^{-1} in March to 0.09 μmol L^{-1} in August in surface waters and from 0.44 μmol L^{-1} in February to 0.78 μmol L^{-1} in August in benthic waters (Fig. 8a). Maximum winter and minimum summer PO_4^{3-} concentrations were similar in all three sub-regions ranging from 0.55–0.67 μmol L^{-1} and 0.06–0.09 μmol L^{-1} respectively (Fig. 9a). PO_4^{3-} measurements from the shelf break region in March were sparse leading to an anomalous and unrealistic decrease of ~0.3 μmol L^{-1} between February and March. Notably, minimum PO_4^{3-} concentrations occur earlier on the shelf in July and one month later in August in shelf break and offshelf waters. The apparent timing of maximum annual PO_4^{3-} concentrations varied more widely occurring in November at the shelf break, in January on the shelf and in March at oceanic stations. The most obvious difference between the three sub-regions therefore was a faster rate of decrease (i.e. shorter time period between maximum and minimum concentrations) and earlier onset of reduction in PO_4^{3-} concentrations on the shelf relative to the shelf break and ocean which is likely connected with earlier bloom onset on the shelf compared to the ocean (Fig. S2). Strong similarities in concentrations and timing at shelf break and oceanic stations support the view that the shelf break is more ocean-like than shelf-like.

Mean monthly Si concentrations ranged from 4.6 μmol L^{-1} in January to 0.38 μmol L^{-1} in August in surface waters and from 3.57 μmol L^{-1} in December to 4.71 μmol L^{-1} in July in benthic waters (Fig. 8b). Benthic Si concentrations varied by only 1.14 μmol L^{-1} across the year with Si being the least variable of the three macronutrients. Maximum winter and minimum summer Si concentrations were similar in the mixed layer of all three sub-regions ranging from 4.26–4.90 μmol L^{-1} and 0.27–0.51 μmol L^{-1} respectively (Fig. 9b). Concentrations were highest between January and March (> 4 μmol L^{-1}), decreased sharply between March and May and remained low (< 1 μmol L^{-1}) throughout the summer with residual concentrations being higher on the shelf than in the ocean. Autumnal mixing in November and December increased concentrations to ~3 μmol L^{-1}, though concentrations remained at intermediate values between the summer minimum and winter maximum concentrations until the onset of winter (i.e. January onwards). It is notable that unlike PO_4^{3-} (or NO_3^-), Si concentrations decreased sharply in spring rather than steadily, and continuously decreasing into summer indicating that most Si utilization is restricted to the spring months only. Si concentrations reduced earlier and faster on the shelf compared to the ocean and shelf break (Fig. 9b). Interestingly, annual minimum Si concentrations were spread over several months occurring in June (shelf break), August (ocean) and October (shelf) suggesting that there may be sub-regional differences in the utilization of Si throughout the year.

Mean monthly NO_3^- concentrations ranged from 8.86 μmol L^{-1} in March to 0.81 μmol L^{-1} in August in surface waters and from 6.01 μmol L^{-1} in January to 11.33 μmol L^{-1} in August in benthic

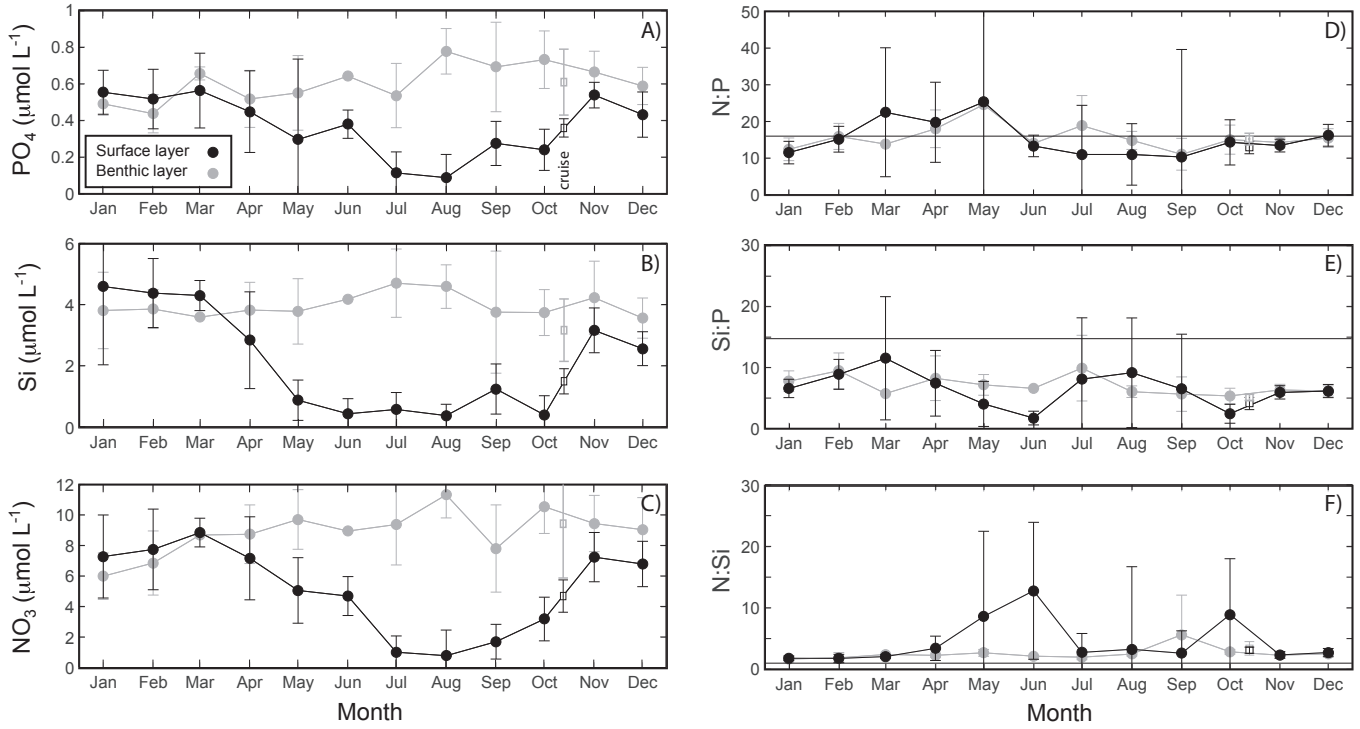

Fig. 8. Mean annual cycles of inorganic nutrient concentrations and nutrient stoichiometries for the Hebrides Shelf region (55–60°N, 7–12°W) for the surface (black line) and benthic (grey line) water column layers based on historical nutrient data for the period 1960–2014. Horizontal black lines denote Redfield stoichiometric ratios based on the standard stoichiometric formula of 106C:15Si:16N:1P. Open black and grey squares indicate the 2014 cruise results for reference (Table 1).

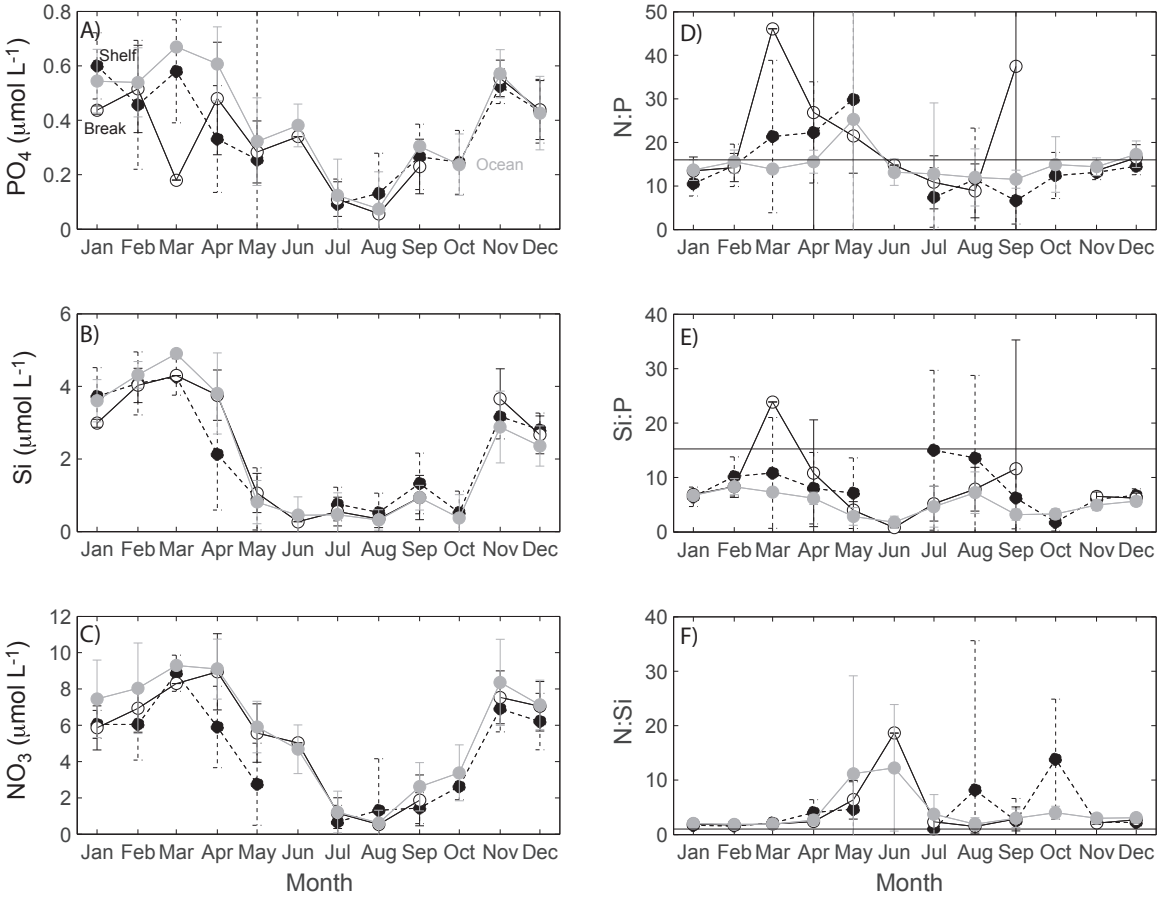

Fig. 9. Mean annual cycles of inorganic nutrient concentrations (left hand column) and nutrient stoichiometries (right hand column) within the surface layer for the shelf (black dashed line, black circles), shelf break (black solid line, open circles) and ocean (grey line, grey circles) sub-regions of the Hebrides Shelf (55–60°N, 7–12°W) based on historical nutrient data for the period 1960–2014. Note the earlier reduction in nutrient concentrations on the shelf compared to the shelf break and ocean sub-regions. Horizontal black lines denote Redfield stoichiometric ratios based on the standard stoichiometric formula of 106C:15Si:16N:1P.

waters (Fig. 8c). In benthic waters a slow but continuous increase in NO_3^- concentrations between January and August was followed by a small decrease between September and December most likely due to vertical mixing. Similar, sub-regional winter maximum and summer minimum NO_3^- concentrations were observed in surface waters with ranges of 8.87–9.3 μmol L^{-1} and 0.54–0.68 μmol L^{-1} respectively (Fig. 9c). Concentrations were highest during late autumn and winter (November to March), decreased gradually between March and July and generally remained low (< 2 μmol L^{-1}) during summer (July-September), before increasing during autumn. Subtle differences in the annual cycle of NO_3^- compared to PO_4^{3-} and Si were evident which may reflect both the intensity of vertical mixing, wind-driven cross-shelf exchange with the neighbouring North Atlantic Ocean, preferential nutrient remineralization rates or potential nutrient sources on the shelf. For example, NO_3^- concentrations reduced faster and earlier on the shelf than elsewhere with the main drawdown occurring between March and July. Also, the annual cycle in NO_3^- concentrations on the shelf was distinct from that of the shelf break and neighbouring ocean, despite similar ranges in nutrient concentrations over the year.

NO_3^-:PO_4^{3-} varied from a minimum of 10.3 in September to a maximum of 25.3 in May in surface waters (Fig. 8d). NO_3^-:PO_4^{3-} above 16:1 occurred between March and May and in December only and was below 16:1 for the rest of the year. The greatest variability in the NO_3^-:PO_4^{3-} ratio was seen in May and September. The NO_3^-:PO_4^{3-} of the benthic layer ranged from 24.6 in May to 11.1 in September (Fig. 8d). Excluding the value for May, which has a large standard deviation associated with it, NO_3^-:PO_4^{3-} was broadly stable across the year ranging from 11.1 to 18.9. Only the months of April, May and July displayed NO_3^-:PO_4^{3-} > 16, thus the benthic layer was predominately PO_4^{3-} rich relative to NO_3^-. The three sub-regions displayed broadly similar but not identical stoichiometric characteristics. NO_3^-:PO_4^{3-} typically reached its annual maximum in the spring between March (shelf break) and May (shelf & ocean) but varied in magnitude from 25.3 – 46.1 whilst annual minimum NO_3^-:PO_4^{3-} occurred in summer between August (shelf break) and September (shelf & ocean) with similar values ranging from 6.6 to 11.6 (Fig. 9d). NO_3^-:PO_4^{3-} exceeded 16:1 in spring between March and May, but whereas the shelf and shelf break regions displayed elevated NO_3^-:PO_4^{3-} for all of this period the oceanic NO_3^-:PO_4^{3-} was only elevated in May. In fact May was the only month of the year that the oceanic NO_3^-:PO_4^{3-} was > 16, suggesting that offshelf surface waters were not only comparatively PO_4^{3-} rich (relative to NO_3^-) throughout the year but most likely a significant source of PO_4^{3-} to the shelf break and shelf regions later in the year.

Surface Si:PO_4^{3-} ranged from 1.7 in June to 11.5 in March with the greatest change occurring over a 4 month period coincident with the spring bloom (Fig. 8e). Benthic Si:PO_4^{3-} meanwhile ranged from 9.9 in July to 5.3 in October but more generally decreased throughout the year with highest Si:PO_4^{3-} in winter and spring and lowest values in summer and autumn. The ratio for July was associated with a high standard deviation thus July appeared outside of the general annual trend. Generally, the benthic layer was Si rich relative to PO_4^{3-} (Fig. 8e). However, the annual trend in Si:PO_4^{3-} was driven by a comparatively larger increase (77%) in benthic layer PO_4^{3-} concentrations rather than changes in the Si pool (32%). A distinction could be made between the shelf and the shelf break and ocean sub-

regions due to elevated Si:PO_4^{3-} on the shelf throughout spring and summer (Fig. 9e). Across the region (Fig. 8e), Si:PO_4^{3-} displayed two maxima, one in March (end of winter) and one in August (summer) due to the shelf break and ocean sub-regions both displaying an annual minimum in June (Fig. 9e). Si:PO_4^{3-} on the shelf diverged from that of the shelf break and ocean sub-regions between May and September due to higher Si and lower PO_4^{3-} concentrations on the shelf at this time relative to the ocean. Between July and September the majority of nutrient observations were made on the shelf thus the August Si:PO_4^{3-} maximum and the large variability associated with the monthly mean values for these months reflects increased variability in the nutrient stoichiometry of shelf waters rather than a general resupply of Si (or removal of PO_4^{3-}) as both Si and PO_4^{3-} concentrations were broadly constant over these months (Fig. 9a, 9b).

NO_3^-:Si ranged from 1.8 in February to 12.8 in June in surface waters signifying that NO_3^- was more abundant than Si throughout the year (maximum and minimum NO_3^- concentrations were ~2-fold higher than Si) (Fig. 8f). Thus to first order the Hebrides Shelf may be viewed as a Si limited system. There was one major peak in the NO_3^-:Si ratio during May and June, and a second minor peak in October with low values in July and August. The peak in May-June was driven by the rapid removal of Si relative to NO_3^- at this time, whilst the peak in October was apparently driven by a replenishment of NO_3^- but not Si in surface waters. In the benthic layer NO_3^-:Si ranged from 1.7 in January to 5.6 in September, thus NO_3^-:Si tended to increase throughout the year (Fig. 8f). Despite good spatial coverage the mean NO_3^-:Si for September had a large standard deviation associated with it indicating significant variability within the data for this month. Mean benthic layer NO_3^- concentrations also appeared lower than expected for September (Fig. 8c) so if September is excluded, the annual range in NO_3^-:Si reduced to between 1.7 and 2.9, suggesting that benthic layer NO_3^-:Si was rather invariant over the year. Interestingly, NO_3^-:Si remained above 1 throughout the year signifying the persistence of NO_3^- rich water across the shelf. Differences in NO_3^-:Si between the shelf break and ocean were small compared to the shelf region which displayed the largest variability of the three sub-regions (Fig. 9f). The highest NO_3^-:Si of 18.6 was observed in June at the shelf break.

The stoichiometric character of the Hebrides Shelf surface waters are summarised via a nutrient ratio:ratio plot (Fig. 10a). This showed that the region has a broadly balanced provision of NO_3^- and PO_4^{3-} in winter and late autumn, shifts strongly towards PO_4^{3-} deficiency relative to NO_3^- in spring and persistent Si deficiency relative to NO_3^- from spring onwards, and then experiences widespread NO_3^- deficiency relative to PO_4^{3-} and Si deficiency relative to PO_4^{3-} during the summer. There is greater stoichiometric variability in the summer months (August-September) than at any other time of year suggesting widespread and variable potential for nutrient limitation at this time due to seasonal stratification and isolation of surface waters from deeper nutrient reservoirs. Furthermore, the variable stoichiometry during summer suggests patchy nutrient distributions at this time. The nutrient ratio:ratio plot for the benthic layer revealed modest variability over the year with NO_3^-:PO_4^{3-} > 16:1 from April to July (Fig. 10b). Compared to surface waters the observations were tightly clustered showing less variation in the NO_3^-:PO_4^{3-}, Si:PO_4^{3-} or NO_3^-:Si ratios except in autumn when a small cluster of datapoints emerged showing low Si:PO_4^{3-} thus overall there was weaker seasonality present in the benthic data.

3.3.2. Organic nutrient analysis

3.3.2.1. Seasonal organic nutrient concentrations. Mean regional surface (0–30 m) DOC concentrations ranged from an autumn minimum of 63.9 ± 7.7 μmol L^{-1} to a summer maximum of 81.1 ± 7.7 μmol L^{-1}, an increase of ~ 17 μmol L^{-1} over the year (Table 3). DON concentrations were also highest in summer (6.5 ± 2.0 μmol L^{-1}) and lowest in autumn (4.7 ± 1.0 μmol L^{-1}). DOP data were absent for autumn and winter, but concentrations were higher in summer (0.14 ± 0.09) than in spring (0.09 ± 0.08). The organic pools were therefore all largest in summer and most likely at their smallest in autumn. Mean annual concentrations of DOC, DON and DOP were 70.6 ± 10.8 μmol C L^{-1}, 5.70 ± 2.5 μmol N L^{-1}, and 0.12 ± 0.09 μmol P L^{-1} respectively. The data were inadequate to fully characterise seasonality in the organic nutrient pool stoichiometry due to the lack of DOP data but coverage was sufficient to reveal that the DOC:DON was < 16 in all seasons (range of 11.1:1 to 13.7:1; Table 3) and therefore similar to the average for marine waters of 13.6:1 (Benner, 2002). The mean annual C:N:P ratio within surface waters of 588C:48N:1P indicated a carbon and nitrogen rich nutrient pool (relative to the Redfield ratio). Compared to marine bulk DOM,

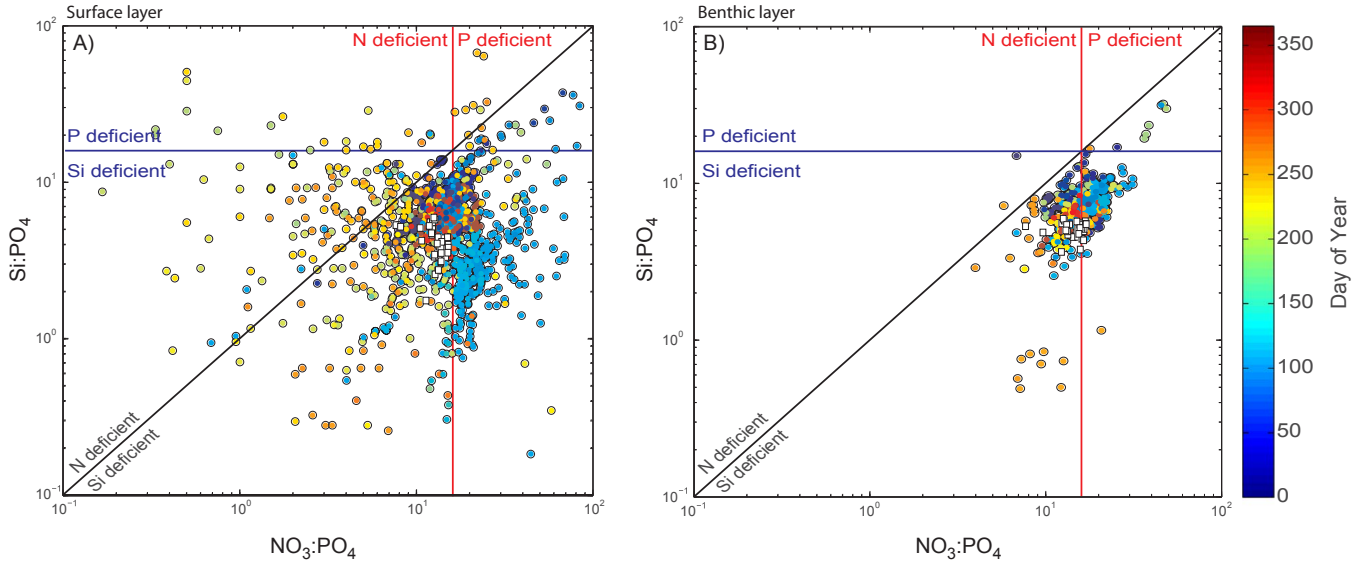

Fig. 10. Nutrient ratio-ratio plots for a) the surface layer and b) the benthic layer revealing the cyclical nature of seasonal perturbations to the stoichiometry of the inorganic nutrient pool for the Hebrides Shelf. Results are based on the analysis of historical nutrient data (1960–2014). The vertical red lines, horizontal blue lines and diagonal black lines represent Redfield stoichiometric ratios based on the standard stoichiometric formula of 106C:15Si:16N:1P. Note the existence of similar seasonal perturbations in both layers but the reduced magnitude of these perturbations in the benthic layer. Cruise data from Fig. 3 are included for comparison and indicated by white squares. (For interpretation of the references to colour in this figure legend, the reader is referred to the web version of this article.)

Table 3
Mean (± s.d.) seasonal organic nutrient concentrations (μmol L^{-1}) and stoichiometries (molar) for the Hebrides Shelf region (52–60°N) and for the shelf, shelf break and ocean sub-regions. Seasonal means are based on available literature data within a 0–30 m surface layer and a 30–300 m (or seabed if shallower) benthic layer with the sub-region identified via a simple bathymetric criteria (see text). Mean annual concentrations and layer differences are also presented for the region and sub-regions. Elemental ratios are based on mean seasonal concentrations where possible.

Sub-region	Parameter	Winter (JFM)		Spring (AMJ)		Summer (JAS)		Autumn (OND)		Annual		
	Layer	Surface	Benthic	Surface	Benthic	Surface	Benthic	Surface	Benthic	Surface	Benthic	% difference
Shelf	DOC	70.04 ± 11.11	68.1 ± 10.56	66.73 ± 5.49	61.84 ± 8.85	82 ± 3.61	82.67 ± 3.21	63.04 ± 1.84	59.14 ± 2.89	68.82 ± 9.26	65.51 ± 10.43	-4.80
	DON	5 ± 3.27	6.55 ± 9.8	9.75 ± 6.24	4.98 ± 1.14	7.01 ± 1.32	4.5 ± 1.36	5.06 ± 0.61	5.13 ± 0.32	6.21 ± 3.85	5.66 ± 6.51	-8.81
	DOP	–	–	0.09 ± 0.08	0.04 ± 0.02	–	–	–	–	0.09 ± 0.08	0.04 ± 0.02	-55.56
	DOC:DOP	–	–	741.4	1546.0	–	–	–	–	764.7	1637.8	
	DON:DOP	–	–	108.3	124.5	–	–	–	–	69.0	141.5	
	DOC:DON	14.0	10.4	6.8	12.4	11.70	18.37	12.46	11.53	11.1	11.6	
Break	DOC	64.58 ± 5.31	63.16 ± 3.45	64 ± 8.49	68 ± 7.43	84.54 ± 10.02	80.46 ± 12.27	64.61 ± 8.52	65.76 ± 8.47	73.25 ± 13.19	72.26 ± 11.99	-1.35
	DON	7.65 ± 0.89	7.78 ± 0.73	3.17 ± 1.11	2.85 ± 0.61	7.76 ± 2.4	5.04 ± 2.09	4.92 ± 1.06	4.86 ± 1.7	6.48 ± 2.42	5.36 ± 2.19	-17.35
	DOP	–	–	0.07 ± 0.08	0.06 ± 0.02	0.18 ± 0.11	0.15 ± 0.06	–	–	0.14 ± 0.11	0.12 ± 0.07	-14.88
	DOC:DOP	–	–	914.3	1133.3	469.7	536.4	–	–	523.2	602.2	
	DON:DOP	–	–	45.3	47.5	43.1	33.6	–	–	46.3	44.7	
	DOC:DON	8.4	8.1	20.2	23.9	10.9	16.0	13.1	13.5	11.3	13.5	
Ocean	DOC	65.64 ± 8.89	69.82 ± 17.4	72.26 ± 9.14	69.1 ± 7.6	78.67 ± 5.2	69.31 ± 6.49	63.86 ± 8.56	59.29 ± 6.45	70.04 ± 10	65.85 ± 10.47	-5.98
	DON	6.29 ± 2.34	7.38 ± 1.44	4.72 ± 1.57	3.84 ± 1.12	5.68 ± 1.2	4.1 ± 2.06	4.45 ± 1.01	3.47 ± 1.16	5.21 ± 1.65	4.46 ± 2.08	-14.37
	DOP	–	–	0.1 ± 0.09	0.08 ± 0.05	0.14 ± 0.09	0.09 ± 0.07	–	–	0.12 ± 0.09	0.09 ± 0.07	-24.77
	DOC:DOP	–	–	722.6	863.8	561.9	770.1	–	–	583.7	731.7	
	DON:DOP	–	–	47.2	48.0	40.6	45.6	–	–	43.4	49.6	
	DOC:DON	10.4	9.5	15.3	18.0	13.9	16.9	14.4	17.1	13.4	14.8	
All regions	DOC	67.07 ± 9.34	68.09 ± 13.77	68.95 ± 8.45	66.86 ± 8.34	81.1 ± 7.65	73.53 ± 10.19	63.89 ± 7.65	60.09 ± 6.67	70.59 ± 10.78	67.16 ± 11.07	-4.86
	DON	6.04 ± 2.67	7.2 ± 5.37	5.61 ± 3.74	4.01 ± 1.24	6.52 ± 1.95	4.46 ± 2.06	4.65 ± 0.98	3.79 ± 1.32	5.7 ± 2.45	4.84 ± 3.24	-15.05
	DOP	–	–	0.09 ± 0.08	0.07 ± 0.05	0.14 ± 0.09	0.11 ± 0.07	–	–	0.12 ± 0.09	0.09 ± 0.07	-23.58
	DOC:DOP	–	–	766.1	955.1	579.3	668.5	–	–	588.3	746.2	
	DON:DOP	–	–	62.3	57.3	46.6	40.5	–	–	47.5	53.8	
	DOC:DON	11.1	9.5	12.3	16.7	12.4	16.5	13.7	15.9	12.4	13.9	

Table 4
Estimates of benthic layer nutrient remineralization based on measured apparent oxygen utilization (AOU) rates and stoichiometric assumptions from Redfield et al. (1963), Anderson (1995) and this study (150C:7Si:18N:1P:-150O_2). For each region we present the mean (± s.d.) dissolved oxygen concentration, mean saturated oxygen concentration at in-situ temperature and salinity, mean AOU rate, mean concentration of remineralized nutrient (NO_3, PO_4, Si, and DIC) and the percentage of the mean benthic in-situ nutrient pool (Table 1) represented by the mean remineralized nutrient concentration.

Layer	Region	In-situ oxygen (μmol L^{-1})	Saturated oxygen (μmol L^{-1})	AOU (μmol L^{-1})	Stoichiometric assumption	Remineralized contribution (μmol L^{-1})				% of measured benthic pool			
						NO_3 (μmol L^{-1})	PO_4 (μmol L^{-1})	Silicate (μmol L^{-1})	CO_2	NO_3	PO_4	Si	DIC
Benthic layer	Shelf	255.4 ± 15.4	271.4 ± 4.9	-16.0 ± 19.7	*Redfield*	1.86	0.12	1.74	12.31	26.0	23.2	66.0	0.56
					Anderson	1.71	0.11	1.60	11.32	23.9	21.4	60.7	0.52
					This study	1.92	0.11	0.75	16.02	26.9	21.4	28.3	0.73
	Shelf break	260.2 ± 5.2	277.1 ± 2.2	-16.9 ± 7.0	*Redfield*	1.96	0.12	1.83	12.97	16.4	16.5	49.2	0.59
					Anderson	1.80	0.11	1.69	11.93	15.1	15.2	45.3	0.54
					This study	2.03	0.11	0.79	16.88	17.0	15.2	21.1	0.76
	Ocean	274.9 ± 3.1	278.1 ± 1.5	-3.3 ± 3.0	*Redfield*	0.38	0.02	0.35	2.49	3.2	3.3	9.4	0.11
					Anderson	0.35	0.02	0.32	2.29	2.9	3.0	8.7	0.10
					This study	0.39	0.02	0.15	3.25	3.3	3.0	4.1	0.15
	All	263.0 ± 13.9	274.8 ± 4.8	-11.8 ± 15.0	*Redfield*	1.37	0.09	1.28	9.06	14.5	14.0	40.6	0.41
					Anderson	1.26	0.08	1.18	8.33	13.4	12.9	37.3	0.38
					This study	1.42	0.08	0.55	11.79	15.0	12.9	17.4	0.54

which has a mean composition of 300C:22N:1P (Benner, 2002), the mean annual ratio indicated a higher C and N content relative to P but a ratio of DOC:DON comparable to the average for marine waters (12.4:1 vs 13.6:1).

Mean regional benthic DOC concentrations ranged from an autumn minimum of 60.1 ± 6.7 μmol L^{-1} to a summer maximum of 73.5 ± 10.2 μmol L^{-1}, an increase of ~ 13 μmol L^{-1} over the year (Table 3). DON concentrations were highest in winter (7.2 ± 5.4 μmol L^{-1}), and lowest in autumn (3.8 ± 1.3 μmol L^{-1}). DOP data was again absent for autumn and winter but maximum concentrations occurred in summer (0.11 ± 0.07 μmol L^{-1}). Given the similar timings of seasonal maximum/minimum concentrations for surface and benthic waters the atypical timing of the benthic DON winter maximum is curious. Interestingly the seasonal DOC:DON was ~16 for all seasons except winter when it was lower on account of the elevated mean DON concentration. The mean annual benthic C:N:P was 746C:54N:1P and therefore larger than the global mean of 330C:22N:1P (Benner, 2002). On an annual basis the mean benthic layer concentrations of DOC, DON and DOP were 5%, 15% and 24% lower than in the surface layer revealing a preferential removal of P relative to N and of N relative to C with depth.

3.3.2.2. Sub-regional organic nutrient concentrations. All sub-regions displayed similar seasonal patterns and broadly similar seasonal concentrations to the regional mean described above albeit with some important differences (Table 3). For example, DOC concentrations varied by 19–20 μmol L^{-1} over the year at the shelf break and on the shelf, but by only 15 μmol L^{-1} offshelf. Similarly the annual range in DON and DOP measurements was smaller offshelf (2.45 μmol N L^{-1} and 0.04 μmol P L^{-1}) than on the shelf (4.75 μmol N L^{-1} and 0.05 μmol P L^{-1}). However, on an annual basis mean surface organic nutrient concentrations were higher at the shelf break than on the shelf or offshelf. In the case of DOC this appears to be driven by a higher mean summer concentration (84.6 ± 10.0 μmol L^{-1}) and a near constant mean concentration of ~64 μmol L^{-1} during all other seasons, whereas the shelf and ocean sub-regions displayed greater seasonal variability. Seasonal maximum DON concentrations were more variable between sub-regions and peaked in winter in the ocean, in spring on the shelf and in summer at the shelf break. DOP concentrations were highest in summer and the data indicated a higher summer maximum at the shelf break compared to the ocean. Summer DOP data are absent for the shelf. Consequently, the lack of summer DOP measurements for the shelf led to an elevated mean annual C:N:P on the shelf (765C:69N:1P) compared to the shelf break (523C:46N:1P) and ocean (584C:43N:1P).

Split by layer mean annual benthic DOC concentrations were 5%, 1% and 6% lower for the shelf, shelf break and ocean sub-regions. DON concentrations were 9%, 17% and 14% lower and DOP concentrations were 56%, 15% and 25% lower for the shelf, shelf break and ocean sub-regions respectively. There was thus stronger phosphorous removal relative to nitrogen and carbon in the benthic waters of all three sub-regions, but particularly on the shelf. Collectively the data show that organic nutrient concentrations decrease with depth but that P is removed more strongly than N and N removed more strongly than C elevating the organic nutrient pool stoichiometry of the deeper waters.

3.4. Apparent oxygen utilization and nutrient remineralization

Apparent oxygen utilization rates provide valuable insight into remineralization rates in deep waters, a process that will ultimately impact the nutrient stoichiometry at depth (Anderson and Sarmineto, 1994; Thomas, 2002). However, in shallow and dynamic coastal waters the interpretation of AOU rates can be complicated due to multiple factors impacting oxygen concentrations (Topcu and Brockmann, 2015). Nevertheless, prior to the destruction of a stratified water column in winter, benthic AOU rates should provide a useful approximation of respiration occurring beneath the mixed layer.

Within the cruise dataset there was a clear signature of biological production in the surface mixed layer resulting in a positive AOU of between 9.7 and 13.7 μmol L^{-1}. A seaward increase in AOU rates indicated stronger productivity offshelf (Table 4) but salinity changes may also be relevant in driving this gradient (Testa and Kemp, 2011). Benthic layer AOU rates strongly decreased from -3.3 μmol L^{-1} offshelf to -16.9 μmol L^{-1} at the shelf break and -16 μmol L^{-1} on the shelf, with the implication being stronger benthic oxygen consumption on the shelf than in the ocean. This was due, in part, to a shallow water column trapping the product of a highly productive shelf system compared to the ocean where organic material will continue to settle to the deep ocean seafloor (> 2500 m in the Rockall Trough region of this study) and be remineralized at deeper depths than considered here.

Estimates of nutrient remineralization determined from AOU rates using the Redfield stoichiometric formula (106C:15Si:16N:1P:-138O_2; Redfield et al., 1963) and the modified Anderson formula (106C:15Si:16N:1P:-150O_2; Anderson, 1995) for typical marine organic matter were compared to remineralization estimates derived using the mean particulate stoichiometry reported here (150C:7Si:18N:1P:-150O_2; where we assume the same oxygen content as Anderson, 1995) to determine the magnitude of error involved in using a fixed stoichiometry. It is now generally acknowledged that the Redfield ratio underestimated the O_2 content of organic matter, which can subsequently overestimate the oxidation of organic matter and the release of nutrients from measured AOU rates. The revised oxidation ratios presented by Anderson (1995) correct for this. Despite the importance of correctly accounting for the O_2 content of organic matter, in this analysis final differences of < 5% (as a proportion of the remineralized benthic nutrient pool) were found between these two widely used stoichiometric ratios implying minor but important distortions could arise from use of one ratio in favour of the other.

Estimates of the amount of carbon dioxide, silicate, nitrate and phosphate released from remineralized organic material based on the measured AOU rates are presented in Table 4. Under the Redfield formulation the mean remineralized contribution to the benthic layer nutrient pool was 9.1, 1.3, 1.4 and 0.09 μmol L^{-1} for carbon dioxide, silicate, nitrate and phosphate respectively, representing 0.4%, 41%, 15% and 14% of mean benthic layer nutrient concentrations. Under the Anderson formulation the mean contributions reduced slightly to 8.3, 1.2, 1.3 and 0.08 μmol L^{-1} for carbon dioxide, silicate, nitrate and phosphate respectively, representing 0.4%, 37%, 13% and 13% of mean benthic layer nutrient concentrations. Silicate remineralization was by far the most significant term with 37–41% of the benthic silicate pool potentially sourced from the remineralization of organic matter sinking from the surface waters above. Silicate was also the most sensitive to the varying O_2 content of the stoichiometric formulae. In contrast ~14% of benthic nitrate and phosphate concentrations may have been attributable to local remineralization processes.

Use of the mean stoichiometric ratios obtained in this study suggest 11.8, 0.6, 1.4 and 0.08 μmol L^{-1} of carbon dioxide, silicate, nitrate and phosphate may have been supplied, representing 0.5%, 17%, 15% and 13% of benthic layer nutrient concentrations. The largest resulting differences between the three stoichiometric assumptions therefore are in the quantity and proportion of silicate that could be remineralized (Table 4).

Spatial heterogeneity in AOU rates was also important with the higher AOU rate on the shelf potentially accounting for 24–27%, 28–66%, 21–23% and 0.5–0.7% of measured benthic layer nitrate, silicate, phosphate and DIC concentrations whilst the lower oceanic AOU rate accounted for 3%, 4–9%, 3% and 0.1–0.2% of the measured nitrate, silicate, phosphate and DIC pools. The shelf break assumed an intermediate position with 15–17%, 21–49%, 15–16% and 0.5–0.8% of the measured nitrate, silicate, phosphate and DIC pools potentially being attributable to localised remineralization (Table 4).

3.4.1. Remineralization contribution to layer differences

An alternative approach based on differences in nutrient concentrations between the mixed layer and benthic layer, rather than the absolute benthic layer nutrient concentrations, may be more appropriate for identifying the true significance of remineralization due to weak cross-shelf exchange (Booth and Ellett, 1983; Huthnance, 1986; Souza et al., 2001), an approximate 9 month residence time for this shelf (Prandle, 1984; McKay et al., 1986; McCubbin et al., 2002), and strong vertical partitioning of the water column over seasonal timescales. On the shelf benthic DIC concentrations were on average 23.6 μmol L^{-1} higher than in the surface mixed layer (Table 1; note however that there was also considerable variability between stations). Thus based on a shelf mean AOU rate of -16.0 μmol L^{-1} (Table 4), and the Anderson stoichiometric formulation approximately 11 μmol L^{-1} (48%) of the vertical increase may have originated from localised oxidation of organic matter. At the shelf break the mean difference between surface and benthic layer DIC concentrations was 41.7 μmol L^{-1} and 11.9 μmol L^{-1}, or 29% of the increase in the benthic layer could have been accounted for via organic matter remineralisation. Offshelf the DIC concentration increased by an average of 32.7 μmol L^{-1} between the surface mixed layer and benthic layer and 2.3 μmol L^{-1} or 7% of the increase in DIC with depth could have been attributable to remineralization. The seaward decrease in the proportion of the benthic layer DIC pool attributable to local remineralization is most likely due to proximity to the deep ocean DIC reservoir, but water column depth likely plays an important role. Similar patterns were identified for both NO_3^- and PO_4^{3-} with 47%, 26% and 5% of benthic layer NO_3^- and 53%, 30% and 6% of benthic layer PO_4^{3-} pools in shelf, shelf break and oceanic sub-regions potentially attributable to remineralization. The greater proportions of benthic layer PO_4^{3-} attributable to local remineralization compared to NO_3^- implies preferential recycling of P relative to N in a shelf sea setting which is generally supported by the other data presented here, particularly the seasonal cycles of DOP and PO_4^{3-}.

Interestingly, in the case of silicate up to 131%, 69% and 13% of benthic layer Si pools for the shelf, shelf break and ocean sub-regions could have been supplied from local remineralization. These simple calculations clearly indicate a larger potential supply of silicate to shelf benthic waters than actually measured due to use of a mean organic matter stoichiometry (Anderson, 1995) that did not reflect the particulate stoichiometry observed. In particular the observed particulate bSi:POP content was typically one-half (~7:1) of that indicated by the traditional Redfield ratio (Fig. 5d). The mean mixed layer particulate stoichiometries on the shelf and at the shelf break were similar with elevated C:P and N:P but depleted Si:P compared to the Redfield/Anderson ratio (148C:7Si:18N:1P vs 142C:8Si:18N:1P vs 106C:15Si:16N:1P; Table 2). Thus, when the assumed C:P, N:P and Si:P of 106:1, 16:1 and 15:1 were replaced with the mean observed C:P, N:P and Si:P of 150:1, 18:1 and 7:1 respectively the recalculated AOU derived nutrient supply could account for 16.0 μmol L^{-1} or 68% of the mean DIC increase of 23.6 μmol L^{-1} within the shelf benthic layer. Similarly 52%, 53% and 61% of shelf benthic NO_3^-, PO_4^{3-} and Si concentrations could have originated from remineralization of organic matter with a mean elemental composition similar to that measured within the surface mixed layer. Remineralization contributions fell sharply at the shelf break to 30%, 30% and 32% of benthic NO_3^-, PO_4^{3-} and Si concentrations due to higher nutrient concentrations at the shelf break. Offshelf the potential contributions were reduced further to ~6% for all nutrients.

3.5. Particulate analysis

3.5.1. Comparison to previous studies

The relationship between carbon, silicate, nitrogen and

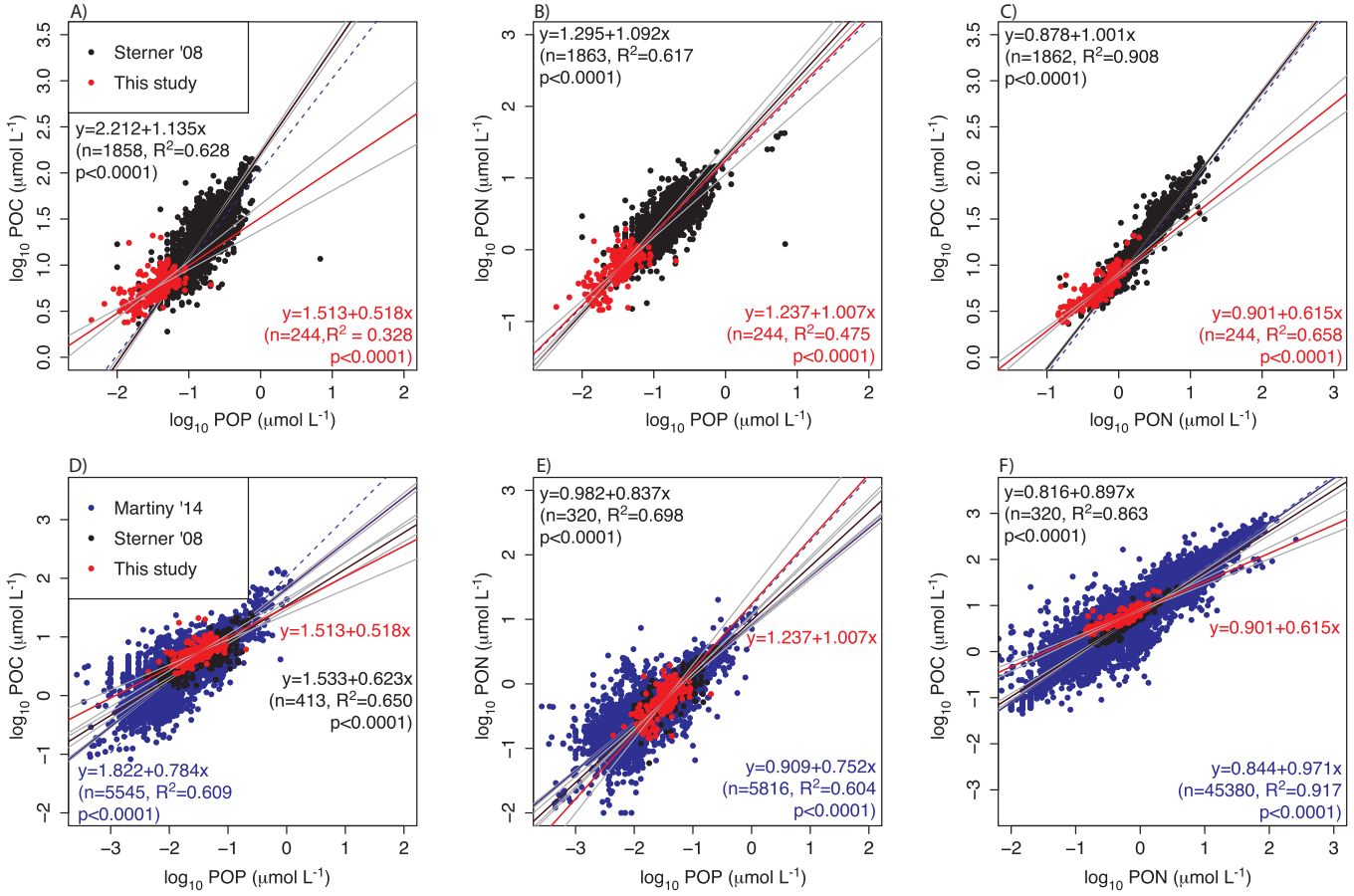

Fig. 11. Comparison of the October-November 2014 particulate data with two similar particulate databases reported by Sterner et al. (2008) and Martiny et al. (2014). In all plots we show Type II major axis regressions (coloured by dataset) with 95% confidence intervals (grey lines) in relation to Redfield relationships (dashed blue lines) through particulate data that has been $\log_{10}$ transformed. In the upper row we compare the Hebrides Shelf data (red) to the coastal dataset (black) collated by Sterner et al. (2008). In the lower row we compare the Hebrides Shelf data (red) against the oceanic datasets of Sterner et al. (2008) (black) and Martiny et al. (2014) (blue). (For interpretation of the references to colour in this figure legend, the reader is referred to the web version of this article.)

phosphorous in particulate organic material is central to the stoichiometric themes explored here. The reliability of the derived stoichiometric relationships were assessed via log–log plots of the entire particulate dataset collected in this study (section 3.1.2) in comparison to other publically available datasets. For the coastal ocean we have incorporated the dataset of POC, PON and POP measurements compiled by Sterner et al. (2008; hereafter S08), and for the open ocean, the dataset reported by Martiny et al. (2013, 2014; hereafter M14) and a smaller oceanic dataset also reported by Sterner et al. (2008).

For the coastal ocean comparison a significant difference in the relationship between carbon and phosphorous and between carbon and nitrogen was found between the Hebrides and S08 datasets (Fig. 11a, c). In both cases the Hebrides dataset deviated away from the Redfield ratio at low particulate concentrations resulting in elevated C:P and C:N values (i.e. high C content; Fig. 5). As a result the linear regressions through the datasets report rather different relationships. As the Hebrides observations were towards the lower end of values reported in the S08 dataset it is possible that the influence of high C:N and C:P production under seasonally weak productive conditions, or differential remineralization of N and P are resulting in distorted relationships between carbon and nitrogen and carbon and phosphorous. In contrast a strong agreement exists between the two datasets describing the relationship between PON and POP (Fig. 11b) with the regression through the Hebrides dataset almost perfectly matching the Redfield relationship.

The open ocean comparison produced conflicting results. The relationship between POC and POP in the Hebrides dataset was similar to that of the S08 oceanic dataset but both were different to that of the M14 dataset (Fig. 11d). As both the Hebrides dataset and the S08 oceanic dataset were far smaller than the M14 dataset the differences may be indicative of undersampling, seasonal bias or reflect the balance between near coastal and open ocean observations within each dataset. In comparison, the relationships between PON and POP within the S08 and M14 datasets were similar but both were different to the Hebrides dataset, which produced a relationship very similar to the Redfield ratio (Fig. 11e). Finally, the relationship between POC and PON indicated that the M14 dataset produced a mean relationship similar to the Redfield ratio whilst the S08 dataset was very similar but both were clearly distinct from the relationship present in the Hebrides dataset (Fig. 11f). Given the spread of data points within the M14 dataset there is nothing to suggest that particulate concentrations within the Hebrides dataset are atypical thus it is more likely that seasonality may best explain the apparent deviations between datasets, particularly for the autumnal dataset reported here for the Hebrides Shelf region.

4. Discussion

A detailed picture of the internal stoichiometry of the Hebrides Shelf has been presented which revealed strong vertical and horizontal gradients in dissolved nutrient and particulate concentrations and in the elemental ratios of those pools. Collectively the Hebrides data reveal increased C:N, C:P and N:P elemental ratios with depth in particulate, dissolved organic and inorganic nutrient pools due both to the preferential remineralization of P relative to N and of N relative to C and to

the variable biological demand for P, N and C. Similar observations were reported for the dissolved organic nutrient pool on Georges Bank (Hopkinson et al., 1997) and more widely across several shelf and oceanic locations (Hopkinson and Vallino, 2005) suggesting the Hebrides results fit to a common principle of stronger biological N and P recycling but weaker C mineralization (e.g. Officer and Ryther, 1980). Simultaneously, the widespread occurrence of high POC:POP and POC:PON particulate matter, relative to the Redfield ratio, in surface waters during an autumn survey of the Hebrides Shelf and neighbouring ocean may initially be suggestive of N or P deficiency under strict adherence to the Redfield ratio of 106C:16N:1P (Redfield et al., 1963). Such an interpretation is in keeping with the autumnal sampling period when nutrient concentrations were low but beginning to increase (Figs. 3 and 8) and the post-autumn bloom timing of the observations (Fig. S2). However, whilst mixed layer NO_3^-:PO_4^{3-} was < 16:1, indicating PO_4^{3-} depletion relative to NO_3^-, concentrations of both NO_3^- and PO_4^{3-} were above potentially limiting thresholds of ~0.5 μmol NO_3^- L^{-1} (Eppley et al., 1969), and ~0.03 μmol PO_4^{3-} L^{-1} (Riegman et al., 2000; Laws et al., 2011; Grant et al., 2013). Si concentrations were frequently below 2 μmol L^{-1} and thus had the potential to be limiting (Egge and Asknes, 1992; though note that in the mesocosm study of Egge and Asknes diatom dominance could still occur when Si was < 2 μmol L^{-1}), however Siemering et al. (2016) actually report higher diatom abundances onshelf than offshelf during autumn 2014 in response to lower ambient NO_3^-:Si; an attribute related to the higher mean Si concentrations on shelf (Table 1) which may be due to N-poor/Si-rich inputs originating from the acidic Scottish highlands (Tett et al., 2003). Dissolved iron concentrations on the shelf were low at this time with separate measurements from cruises in 2010 showing a decline from > 0.5 nmol L^{-1} in spring (E. Achterberg et al, unpublished data) to 0.043 ± 0.019 nmol L^{-1} in summer (Painter et al., 2014), also possibly explaining the higher residual Si concentrations. Thus, the elevated POC:POP (~150:1) (or POC:PON (~9:1)) found in particulate material was unlikely to represent true nutrient limitation and more likely to be indicative of carbon rich particulate matter being synthesised in the mixed layer with a non-Redfield optimum composition (Geider and La Roche, 2002; Sterner and Elser, 2002; Sterner et al., 2008). Subsequent sinking of this material into the benthic layer would therefore transfer more carbon per unit of N or per unit P than indicated by a Redfield-like assumption of the elemental composition. However, the data also revealed significant variability in particulate elemental ratios between shelf and ocean sub-regions (Table 2), which most likely reflected variability in the strength of synthesis and remineralization processes, differences in nutrient availability, and influence of detrital material (Lancelot and Billen, 1985; Frigstad et al., 2011) as well as coincident shelf-to-ocean changes within the phytoplankton community (Siemering et al., 2016). Separately, the analysis of historical nutrient data for the Hebrides region revealed important seasonality in both organic and inorganic nutrient pools with the prominent summer maximum in organic nutrient concentrations reducing DOC:DOP and DOC:DON (i.e. DOM was comparatively C poor) whilst the summer inorganic nutrient minimum elevated DIC:NO_3 and DIC:PO_4 (i.e. comparatively C rich). There were thus important seasonal stoichiometric variations in the inorganic and organic pools of this shelf sea system. As both pools are exportable to the ocean throughout the year (Wakelin et al., 2012; Painter et al., 2016), as well as being transferable between particulate and dissolved pools (Butler et al., 1979), the implications of this stoichiometric variability on the efficiency of cross shelf export fluxes, that is the amount of C exported per unit N or per unit P, need to be carefully considered.

4.1. Annual nutrient cycle in a shelf sea

Winter convective mixing and phytoplankton nutrient utilisation drive the surface mixed layer nutrient cycle. In contrast, respiratory processes in the sediments and benthic water column including bacterial remineralization of sinking organic matter drive the benthic layer nutrient pattern. The annual cycle of nutrients in the benthic layer however is the reverse of that seen in the surface layer with a summer nutrient maximum in the benthic layer coinciding with a summer nutrient minimum in the surface layer (Fig. 8). Across the year mean benthic PO_4^{3-} concentrations increased by 0.34 μmol L^{-1} (annual maximum minus annual minimum) a relative increase of 77%, Si concentrations increased by 1.14 μmol L^{-1} (32%) and NO_3^- concentrations increased by 5.32 μmol L^{-1} (84%). These increases were all smaller than the corresponding drawdown from the surface layer, which saw PO_4^{3-} concentrations reduce by 0.47 μmol L^{-1} (relative decrease of 84%), Si concentrations reduce by 4.22 μmol L^{-1} (92%) and NO_3^- concentrations reduce by 8.05 μmol L^{-1} (91%). Consequently, nutrient increases in the benthic layer represented 72%, 27% and 66% of surface layer PO_4^{3-}, Si and NO_3^- drawdown respectively. A simple mass balance transfer between the surface and benthic layer nutrient pools cannot therefore account for 73% of Si drawdown, 34% of NO_3^- drawdown and 28% of PO_4^{3-} drawdown from the surface ocean.

It is possible that most Si (as opal) is lost to the sediments or transported downslope. The inference therefore is that a substantial proportion of the Si pool must be lost from the shelf system each year. Thus to first order the cross-shelf resupply of Si from the ocean during winter may be a more significant factor for the subsequent productivity of this shelf than the resupply of NO_3^- or PO_4^{3-}.

In contrast N and P were more efficiently recycled and retained yet although approximately two-thirds of the annual surface layer nutrient decrease can be accounted for by the benthic layer nutrient increase (Fig. 8a,c), approximately one-third of the removed nutrient pool remains unaccounted for. As it is generally thought that little carbon biomass from annual primary production is buried in shelf sediments (< 5%; Thomas et al., 2005) the missing nutrients are most likely transferred to higher trophic levels, transferred to the dissolved organic pool (Butler et al., 1979) or transported offshelf to the adjacent ocean. Estimates of offshelf particulate organic carbon flux reported for this shelf by Painter et al. (2016) equated to 22% of annual primary production, comparable to estimates of ~20% reported for other shelf systems (Mackenzie et al., 2004) but larger than estimates of 10–20% reported for Long Island (Falkowski et al., 1988), ~6% for the eastern North American continental margin (Biscaye et al., 1994; Falkowski et al., 1994) or 6–10% based on global mass balance calculations of coastal exchange (Chen et al., 2003; Chen, 2010). Thus, of the 34% of nitrate drawdown and 28% of phosphate drawdown unaccounted for via a simple mass balance calculation most could be transferred to the continental slope and ocean via the particulate phase. Such a fate is supported by the presence of thick phytodetritus layers on the slope and deep seafloor in this region (Mitchell et al., 1997; Bett, 2001). In contrast, long-term nutrient observations from the English Channel by Butler et al. (1979) clearly show that as NO_3^- and PO_4^{3-} are drawn down by phytoplankton in spring there is a subsequent and similar in magnitude increase in the concentration of DON and DOP in summer thus indicating transference from the inorganic to organic nutrient pools. In the western Irish Sea however Moschonas et al. (2015) found that only 38% of total dissolved nitrogen was transferred to the DON pool between spring and summer. Thus whilst it is possible that the missing NO_3^- (as DON) and PO_4^{3-} (as DOP) remain present in the water column having been transferred to the organic pool significant uncertainty over the magnitude of the transference precludes a definitive answer. Elsewhere, Williams (1995) documented a seasonal change in the concentration of dissolved organic matter (DOM) in coastal waters leading to the accumulation of carbon rich DOM by late summer which may potentially be linked to the production of nutrient poor DOM by phytoplankton under nutrient stress (Kepkay et al., 1993). The analysis of extant organic nutrient data for the Hebrides Shelf region revealed a summer maximum and an autumn minimum in DOC, DON and, most likely, in DOP concentrations (Table 3). Though DOP measurements remain scarce for this shelf, DOP observations from Loch

Creran, a sea loch on the west coast of mainland Scotland, support the timing of a summer maximum and autumn minimum in the annual cycle of DOP (Lønborg et al., 2009). In shelf benthic waters the annual cycle resulted in higher DOC:DON during summer (Table 3), as shown by Williams (1995). At the shelf break and ocean regions however DOC:DOP and DOC:DON decreased in summer, in contrast to Williams (1995), and potentially signifying the influence of nitrate and phosphate inputs to the organic pool via phytoplankton excretion or an oceanic influence. Thus whilst the absolute concentration of organic nutrients may be at a maximum in summer the organic pool becomes comparatively carbon rich on shelf but comparatively carbon poor at the shelf break compared to other seasons. Thus any loss of the organic nutrient pool from the shelf at this time may see more carbon per unit nitrogen or per unit phosphorous lost than at other times of year making the cross-shelf flux comparatively efficient for carbon export.

By autumn dissolved organic nutrient concentrations are at their annual minimum most likely driven by a combination of strong bacterial demand (Joint and Pomroy, 1987) and reduced phytoplankton production of DOM due to seasonal nutrient stress (Kepkay et al., 1993). At the Celtic Sea shelf break Joint et al. (2001) reported a seasonal increase in DOC concentrations from ~64 μmol L^{-1} in winter to ~73 μmol L^{-1} in summer; an average increase of ~8–9 μmol L^{-1} over the year. For the Hebrides Shelf region a mean increase of ~17 μmol L^{-1} from autumn (~64 μmol L^{-1}) to the following summer (~81 μmol L^{-1}; Table 3) has been calculated. Joint et al. (2001) estimated that an 8 μmol L^{-1} seasonal increase in DOC concentration could represent a sink for about 9% of the carbon fixed by phytoplankton over the same time period (estimated as ~94 μmol C L^{-1}). Based on a median annual productivity rate of ~200 g C m^{-2} yr^{-1} for the Hebrides Shelf (derived from the typical productivity range reported by Sharples, 2010) an increase in DOC concentrations of 17 μmol L^{-1} would therefore represent a comparable ~10% of total annual production if averaged over a 100 m thick water column. DOC concentrations for the Hebrides region decreased rapidly from the summer maximum of 81.1 ± 7.65 μmol L^{-1} to the autumn minimum of 63.9 ± 7.65 μmol L^{-1}. As this decrease is based on seasonal averages it therefore occurred over a period of ~90 days. If this decrease were due to biological demand alone (rather than reflecting the true balance between supply and demand, which we cannot quantify) this would imply a mean daily rate of consumption of ~0.19 μmol C L^{-1} d^{-1}. Based on the data presented by Joint et al. (2001) for the Celtic Shelf, which indicated mixed layer bacterial production rates decreasing from ~150 mg C m^{-2} d^{-1} in October to ~10 mg C m^{-2} d^{-1} in December as the surface mixed layer deepened from ~30 to > 100 m, an autumnal (Oct to Dec), mean bacterial production rate averaged over the mixed layer of 0.1 μmol C L^{-1} d^{-1} can be estimated. This is similar though lower than the mean daily DOC consumption rate calculated above of 0.19 μmol C L^{-1} d^{-1}, but given the difference in study location, differences in sampling dates, and assumptions over the time period and nature of the time-varying rate of DOC decrease, the similarity is highly encouraging. Moreover this similarity suggests that an approximate autumnal bacterial productivity rate for the Hebrides Shelf can be obtained based on knowledge of the seasonal removal of DOC with a result that is not greatly dissimilar to the average bacterial production rate of between 0.25 μmol C L^{-1} d^{-1} (Oct) and 0.01 μmol C L^{-1} d^{-1} (Dec) calculated from the data reported by Joint et al. (2001). The presence of active bacterial production coupled with knowledge of bacterial inorganic nutrient demand (Kirchman, 1994, 2000; Fouilland et al., 2007) makes it highly likely that a proportion of the missing N and P may ultimately be found in bacterial biomass in addition to being exported from the shelf in the particulate phase.

Comparisons of the inorganic nutrient seasonal cycle in the surface layer for the shelf and shelf break and ocean sub-regions (Fig. 8) did not reveal significant differences in the magnitude of nutrient drawdown but did show that nutrient drawdown starts earlier and proceeds faster on the shelf compared to the neighbouring ocean. Earlier onset of productivity on shelves compared to neighbouring oceans has long been recognised and is typically linked to earlier stabilization of the water column on the shelf (Colebrook and Robinson, 1965; Robinson, 1970; Colebrook, 1979). Thus the nutrient cycle of the shelf break region, as defined here, was more similar to the ocean than to the shelf. This has long been considered due to the role of the European Slope Current acting as an effective barrier to the direct cross shelf exchange of water (Booth and Ellett, 1983; Huthnance, 1986; Souza et al., 2001; Simpson and McCandliss, 2013). Nevertheless, recharging of the nutrient pools during winter when shelf nutrient concentrations reach similar concentrations to the open northeast Atlantic Ocean (~0.7 μmol PO_4^{3-} L^{-1}, ~5 μmol Si L^{-1}, ~9 μmol NO_3^- L^{-1}; Bot et al., 1996; Hydes et al., 2001), suggests that the shelf Si pool is more dependent upon inputs from the ocean than is the case for N and P pools, which, based on the discussion above, can be largely sustained by internal remineralization and recycling.

4.2. Annual stoichiometry of a shelf sea

The internal stoichiometry of the coastal ocean ultimately provides important information on transformations that occur within it and can lead one to infer the presence/absence of specific processes. However, this is often achieved from a particular point of reference such as the assumption of a fixed stoichiometric framework (e.g. Redfield et al., 1963), which can be used to infer nutrient limitation. What has become clear from the data presented here is that the (pre-determined) assumption of a fixed stoichiometric ratio is highly imprecise, as the stoichiometry varies horizontally from shelf to ocean, vertically from mixed layer to benthic layer and with time over the year. These gradients in dissolved nutrient and particulate pools clearly reflect multiple processes including organic matter synthesis, bacterial remineralization, and nutrient supply thus any inferences from the interpretation of the observed elemental ratios relative to an assumed stoichiometric standard must be carefully considered.

Whilst the mean shelf and shelf break POC:PON ratios were comparable to one another and distinctly lower than measured offshore (Table 2), the mean surface NO_3^- concentration at the shelf break was more comparable to that measured in the adjoining ocean and higher than measured on the shelf (Table 1). Thus, there was a distinct spatial difference and decoupling between a major environmental factor (NO_3^- concentration) and the resulting biological expression (POC:PON ratio) of nutrient availability. Precisely why the shelf break appeared chemically similar to the ocean but shelf break particulate material appeared similar to that on the shelf is unclear, but the offshelf gradient in POC:PON ratios appear to follow the offshelf gradient in DIC:NO_3^- (Table 1) suggesting that the measured POC:PON ratio was largely reflective of the environmental gradient in DIC:NO_3^-, despite non-limiting mixed layer NO_3^- concentrations in all three sampled regions (Table 1). Phytoplankton distributions during the autumn survey revealed a marked community difference between shelf and shelf break locations (Siemering et al., 2016) thus the similarity in particulate matter characteristics in these two regions was not obviously due to widespread similarities in the plankton community. Note however that the phytoplankton abundances reported by Siemering et al. (2016) were considerably lower than those reported previously for the same region and season by Fehling et al. (2012).

POC:POP ratios also exhibited a strong cross shelf gradient indicating increased phosphorous deficiency offshelf comparable to the gradient of increased nitrogen deficiency offshelf. However, vertically there was a difference in the way in which nitrogen and phosphorus behaved. Beneath the surface mixed layer the POC:PON ratio increased from 8.2 to 9.8 indicating the preferential remineralization of nitrogen resulting in increasingly carbon rich particulate material with depth. The POC:POP ratio also increased beneath the mixed layer from 148 to 187 but the increase was proportionately larger than for the change in the POC:PON ratio. Thus vertically PON and POP were preferentially

remineralized faster than POC, and POP was remineralized faster than PON. This observation supports the general interpretation from the nutrient observations (Figs. 2 and 3), which showed that the shelf environment was generally depleted in NO_3^- relative to PO_4^{3-}(low NO_3^-:PO_4^{3-}) which the pattern in the particulate data suggests was due to the faster recycling of phosphorous.

The ratio of bSi to POP was generally lower than estimated from the Redfield/Brzezinski estimate for diatoms of 15:1 (Redfield et al., 1963; Brzezinski, 1985). Diatoms are not a major component of the oceanic or shelf break community of this region during autumn (Fehling et al., 2012; Siemering et al., 2016) most likely explaining the low bulk particulate bSi:POP measured offshelf. Diatoms were however were widely distributed across the shelf in autumn 2014 (Siemering et al., 2016) but bSi:POP was still low on the shelf suggesting weak silicification rates. The elemental composition of bulk particulate material is widely taken as indicative of the elemental composition of bulk autotrophic phytoplankton biomass. However, bulk particulate material can contain autotrophic and heterotrophic plankton species, which have varying elemental compositions, as well as variable quantities of detrital material (Lancelot and Billen, 1985; Frigstad et al., 2011). Thus, measured particulate POC:PON, PON:POP or POC:POP ratios must be carefully considered as bulk particulate elemental composition may not provide an unambiguous indication of the composition of autotrophic biomass. In coastal waters there is likely to be a larger impact from detrital and heterotrophic plankton on the composition of bulk particulate material than in the open ocean. Observations of mixed layer particulate stoichiometry (Fig. 7a, c), support this with a wider range of PON:POP and bSi:POP ratios at shelf stations than at shelf break or oceanic stations. Consequently, the observed difference between autumnal mixed layer nutrient stoichiometry (N-deficient; Fig. 10a) and autumnal particulate stoichiometry (predominately P deficient; Fig. 7a) could be due to the presence of detrital material with a high N:P ratio, due to preferential bacterial remineralization of P, distorting the overall N:P ratios.

That the particulate material of the mixed layer displayed a greater tendency towards P deficiency (58% of samples) than N deficiency (42%) and comparatively broad variability in PON:POP ratios, despite the nutrient data unambiguously revealing N deficiency (NO_3^-:PO_4^{3-} < 16:1; Fig. 3d), and narrow variability in NO_3^-:PO_4^{3-} in all areas, suggests either that the nutrient fields are a poor indictor of the potential for (N or P) nutrient limitation, that the observed particulate elemental composition was set by homeostatic regulation (Sterner and Elser, 2002), set in response to some other environmental variable independent of nutrient concentrations (e.g. light (Leonardos and Geider, 2004; Thrane et al., 2016), or temperature (Thrane et al., 2017)) or that the bulk particulate pool elemental stoichiometry reflected the relative balance of autotrophic, hetrerotrophic and detrital material (Frigstad et al., 2011). Clarity on this matter can be obtained from the results of Ptacnik et al. (2010) who demonstrated that particulate PON:POP ratios are in fact the weakest predictor of autotrophic nutrient limitation in coastal regions due to the mixed contribution of autotrophic, heterotrophic and detrital material within bulk particulate pools. However, Ptacnik et al. (2010) also found that the ratio of dissolved inorganic nitrogen (NO_3^- + NO_2^- + NH_4^+) to dissolved phosphate (PO_4^{3-}) was a comparatively better indicator of nutrient limitation. In this study this was approximated via the NO_3^-:PO_4^{3-} ratio due to an absence of data on NH_4^+ concentrations. However, Ptacnik et al. (2010) also suggest that the NO_3^-:PO_4^{3-} ratio does not simply allow for the identification of N or P limitation around a threshold value of 16:1 due to the transition to N limitation occurring at a lower ratio, and the transition to P limitation occurring at a higher ratio; a conclusion reinforced by the work of Geider and La Roche (2002). Thus, Ptacnik et al. (2010) argue that there is a range of NO_3^-:PO_4^{3-} ratios around the canonical value of 16:1 that may better indicate N and P co-limitation (see also Sterner and Elser (2002) where this is discussed further). Some credence to this viewpoint is provided by the nutrient ratio-ratio plot (Fig. 10), which demonstrated a cyclical and therefore predictable pattern in the stoichiometry of the inorganic nutrient pool. Specifically, the inorganic pool shifts towards a high N:P state in spring when coincidentally Si concentrations typically begin to decrease due to the diatom dominated spring bloom (Fig. 2b; S1b). This change in the stoichiometry of the nutrient pool can only occur if the biological nutrient preference (i.e. uptake or draw-down ratio) differs from that presented in the substrate. Thus low NO_3^-:PO_4^{3-} uptake (analogous to luxury PO_4^{3-} uptake; Geider and La Roche, 2002; Ågren, 2004) in spring by fast growing (diatom) species shifts the inorganic nutrient pool towards a high N:P state whilst high NO_3^-:PO_4^{3-} uptake (luxury NO_3^- uptake) in summer shifts the inorganic nutrient pool back towards a lower N:P state. Coupled with known successional changes in phytoplankton community composition (e.g. Colebrook, 1979) the cyclical pattern in the ambient NO_3^-:PO_4^{3-} suggests that there is an inverse relationship between the inorganic nutrient pool stoichiometry and autotrophic nutrient uptake. This then argues for an increased likelihood of P limitation in spring (due to luxury PO_4^{3-} uptake) when fast growing species dominate the community and of N limitation in summer when slower growing species dominate, comparable to the pattern predicted by Elrifi and Turpin (1985). More recently, Thrane et al. (2017) also identified a temperature induced shift in the limiting N:P ratio such that phytoplankton populations become more prone to N limitation at higher temperatures (i.e. warmer seasons), a result also in agreement with the observations reported here.

In summary, significant variability in the stoichiometry of the major dissolved and particulate pools appears to be a common and widespread feature of this shelf system both spatially and seasonally. Consequently, extrapolations from limited observational datasets using a fixed stoichiometric assumption are likely to lead to significant error. This is an important result because mass balance calculations of coastal ocean carbon fluxes do not normally consider the impact of variable elemental stoichiometry when assessing the trophic status of shelf systems. It is, for example, common practice to estimate the proportion of shelf wide net primary production supported by terrestrially derived P via Redfield scaling arguments (e.g. Smith and Hollibaugh, 1993; Ducklow and McCallister, 2004). As a result, even minor deviations in the C:P ratio could easily introduce errors into conclusions of autotrophy or heterotrophy derived from mass balance approaches.

4.3. Stoichiometry of cross shelf flux

Models and observations show that offshelf carbon fluxes associated with an “Ekman Drain” (Souza et al., 2001; Holt et al., 2009; Huthnance et al., 2009; Simpson and McCandliss, 2013) operating along the Hebrides shelf break are far larger for DIC than DOC and larger for DOC than POC reflecting the hierarchy of pool sizes (DIC > DOC > POC) (Wakelin et al., 2012; Painter et al., 2016). Based on data for the shelf break region in autumn 2014 the stoichiometry of the offshelf inorganic nutrient flux was 2960C:5Si:16N:1P, the particulate flux 260C:12Si:26N:1P, and the mean seasonal organic nutrient flux 381C:40N:1P (Fig. 12). Thus, the inorganic nutrient pool represents the most efficient vector for carbon export, and the particulate pool the last efficient relative to phosphorous. Interestingly however, the same is not the case if nitrogen loss from the shelf is considered (again relative to phosphorous) when the N:P of the pools increases from 16:1 in the inorganic pool, to 26:1 in the particulate pool and to 40:1 in the organic pool, suggesting that nitrogen loss from the shelf via the inorganic pool is the least efficient whilst nitrogen loss via the organic nutrient pool is the most efficient. Consequently, the cross shelf flux of organic nutrients assumes greater significance for longer-term shelf wide productivity as it removes comparatively more nitrogen relative to phosphorous than other pools (note that this does not have to imply greater total N loss via the organic pool).

If the offshelf flux via the Ekman Drain were constant throughout the year the changing stoichiometry of the benthic nutrient pools would become an important factor controlling the efficiency, but not

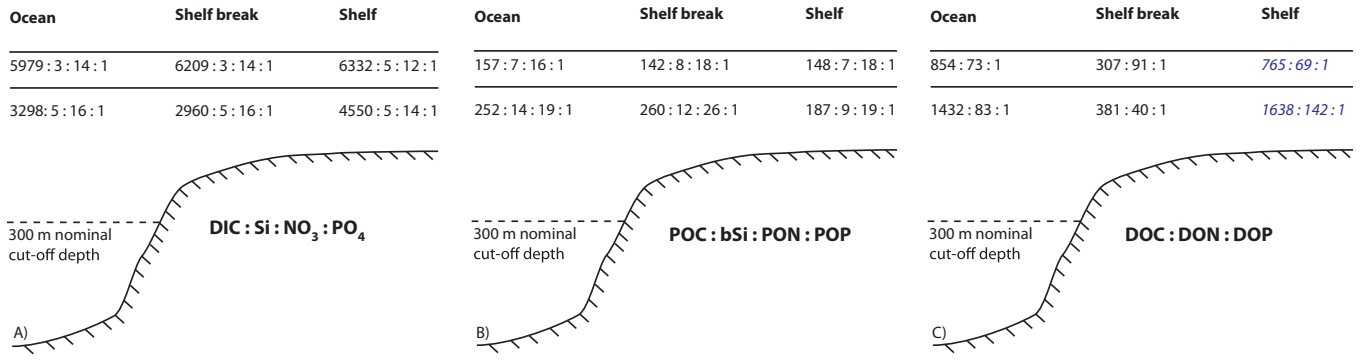

Fig. 12. Mean autumnal stoichiometric patterns of (a) inorganic nutrients, (b) particulate pools and (c) organic nutrients for the surface mixed layer and benthic layers.

magnitude, of the offshelf carbon flux. In reality the Ekman Drain varies seasonally being strongest in winter and weakest in summer due to seasonal changes in the intensity of the northward flowing Slope Current (Dickson et al., 1986; Huthnance, 1986; Carter et al., 1987; Xu et al., 2015). Thus, knowledge of how the stoichiometry of the nutrient pools varies over the year should be more fully incorporated into studies focussed on the offshelf flux of nutrients and the continental shelf pump, as the efficiency of this offshelf flux is a critical aspect of shelf sea biogeochemistry with long-term consequences for the productivity of the shelf region. High efficiency transport (high C:N or C:P) implies internal recycling and retention of N and P elevating the C content of pools, whereas low efficiency (low C:N or C:P) implies long-term loss of N and P from the shelf. Whether there are regional patterns in shelf export efficiency at the global scale remains to be determined.

4.4. Stoichiometric gradients

The internal stoichiometry of the Hebrides shelf during autumn is summarised in Fig. 12. As already described above, there were significant stoichiometric differences within the surface mixed layer and benthic layer between the three pools examined in this study but here the focus is on several notable gradients. For example, within the surface mixed layer DIC:PO_4^{3-} increased towards the coast largely in response to decreased nutrient concentrations on shelf (Table 1). Vertically however, the overall DIC:PO_4^{3-} stoichiometry decreased despite increased DIC concentrations, due to proportionately larger increases in Si, NO_3^- and PO_4^{3-} concentrations with depth than in DIC concentrations (Table 1). NO_3^-:PO_4^{3-} also increased with depth relative to the surface ocean signifying greater NO_3^- availability relative to PO_4^{3-}. In the particulate pools the elemental stoichiometry increased with depth resulting in material that was increasingly C rich relative to N and N rich relative to P signifying that P was remineralized faster than N and N remineralized faster than C. Interestingly the increase with depth differed with proportionately larger increases in elemental stoichiometry at the shelf break and offshelf than on the shelf which may be related to differences in bacterial communities and/or bacterial productivity rates, regional differences in processes that repackage particulate material, or influence from the ocean. It is noteworthy that the highest benthic POC:POP and lowest DIC:PO_4^{3-} were both located at the shelf break suggesting more intense recycling of P here than elsewhere. Finally, the organic pool broadly indicated carbon and nitrogen enrichment with depth, and also relative to the global average ratio of 300C:22N:1P for marine waters (Benner, 2002), once again signifying a remineralization hierarchy of P being remineralized faster than N and of N being remineralized faster than C. However, the limitations of extant organic nutrient measurements, at least for this shelf, prevent more detailed investigation of shelf to ocean gradients.

Stronger remineralization of P relative to N and of N relative to C with depth is now well established (e.g. Hopkinson et al., 1997, 2002; Hung et al., 2003; Lønborg et al., 2009; Lønborg and Alvarez-Salgado, 2012; Davis et al., 2014). This study has shown that this remineralization hierarchy can be found in the inorganic, organic and particulate pools of a temperate latitude shelf sea. It seems less clear from the literature however whether horizontal gradients in remineralization intensity are widespread nor how the presence of such gradients ultimately influences shelf edge export fluxes. This study has shown that horizontal stoichiometric gradients are present, particularly between the shelf and the shelf break, which has implications for the efficiency of shelf sea carbon export, for the effectiveness of N and P retention within the coastal ocean and for longer-term shelf wide productivity. Greater awareness of such gradients and better focus upon the underlying mechanisms creating such gradients may ultimately help reduce the uncertainties associated with cross shelf carbon fluxes and is therefore recommended for future studies.

Acknowledgments

Cruise DY017 was a NERC National Capability funded cruise conducted in support of the UK NERC/DEFRA co-funded Shelf Sea Biogeochemistry programme (NE/K001701/1 and NE/K001884/1). Historical nutrient datasets were obtained from the British Oceanographic Data Centre (www.bodc.ac.uk), Pangaea (www.pangaea.de) and the World Ocean Database (www.nodc.noaa.gov/OC5/WOD/or_wod.html). MODIS Aqua ocean colour observations were obtained from https://oceancolor.gsfc.nasa.gov. L.A. Salt was supported by post-doctoral grants from the Conseil Général du Finistère and Région Bretagne. DY017 cruise datasets are available via www.bodc.ac.uk. We thank the reviewers for their detailed, constructive and helpful comments.

Appendix A. Supplementary material

Supplementary data associated with this article can be found, in the online version, at http://dx.doi.org/10.1016/j.pocean.2017.10.001.

References

Anderson, L.A., Sarmineto, J.L., 1994. Redfield ratios of remineralization determined by nutrient data analysis. Global Biogeochem. Cycles 8 (1), 65–80.
Anderson, L.A., 1995. On the hydrogen and oxygen content of marine phytoplankton. Deep Sea Res. I 42 (9), 1675–1680.
Ågren, G.I., 2004. The C:N:P stoichiometry of autotrophs - theory and observations. Ecol. Lett. 7, 185–191.
Bauer, J.E., Cai, W.-J., Raymond, P.A., Bianchi, T.S., Hopkinson, C.S., Regnier, P.A.G., 2013. The changing carbon cycle of the coastal ocean. Nature 504, 61–70.
Benner, R., 2002. Chemical composition and reactivity. In: Hansell, D., Carlson, C.A. (Eds.), Biogeochemistry of Dissolved Organic Matter. Academic Press, London, pp. 59–90.
Bett, B.J., 2001. UK Atlantic Margin Environmental Survey: Introduction and overview of bathyal benthic ecology. Cont. Shelf Res. 21, 917–956.
Biscaye, P.E., Flagg, C.N., Falkowski, P.G., 1994. The Shelf Edge Exchange Processes experiment, SEEP-II: an introduction to hypotheses, results and conclusions. Deep-Sea Res. II 41 (2/3), 231–252.
Booth, D.A., Ellett, D.J., 1983. The Scottish continental slope current. Cont. Shelf Res. 2

(2/3), 127–146.
Bot, P.V.M., van Raaphort, W., Batten, S., Laanke, R.W.P.M., Philippart, K., Radach, G., Frohse, A., Schultz, H., van den Eynde, D., Colijn, F., 1996. Comparison of changes in the annual variability of the seasonal cycles of chlorophyll, nutrients and zooplankton at eight locations on the northwest European continental shelf (1960–1994). Deutsche Hydrographische Zeitschrift 48 (3/4), 349–364.
Boyer, T.P., Antonov, J.I., Baranova, O.K., Coleman, C., Garcia, H.E., Grodsky, A., Johnson, D.R., Locarnini, R.A., Mishonov, A.V., O'Brien, T.D., Paver, C.R., Reagan, J. R., Seidov, D., Smolyar, I.V., Zweng, M.M., 2013. World Ocean Database 2013. NOAA Atlas NESDIS 72. In: Levitus, S. (Ed.), Mishonov, A. (Technical Ed.). Silver Spring, MD, 209p. http://dx.doi.org/10.7289/V5NZ85MT.
Brzezinski, M.A., 1985. The Si:C:N ratio of marine diatoms: interspecific variability and the effect of some environmental variables. J. Phycol. 21, 347–357.
Butler, E.I., Knox, S., Liddicoat, M.I., 1979. The relationship between inorganic and organic nutrients in seawater. J. Mar. Biol. Assoc. UK, 59, 239–250.
Carter, D.J.T., Loynes, J., Challenor, P.G., 1987. Estimates of extreme current speeds over the continental slope off Scotland. Report No. 239. Institute of Oceanographic Sciences, Wormley, UK, 143p.
Chen, C.-T.A., 2010. Cross-boundary exchanges of carbon and nitrogen in continental margins. In: Liu, K.-K., Atkinson, L., Quinones, R., Talaue-McManus, L. (Eds.), Carbon and Nutrient Fluxes in Continental Margins. Global Change - The IGBP Series. Springer-Verlag, Berlin, pp. 561–574.
Chen, C.-T.A., Liu, K.-K., Macdonald, R., 2003. Continental margin exchange. In: Fasham, M.J.R. (Ed.), Ocean Biogeochemistry. Springer, Berlin, pp. 53–97.
Chen, C.-T.A., Huang, T.-H., Chen, Y.-C., Bai, Y., He, X., Kang, Y., 2013. Air-sea exchanges of CO_2 in the world's coastal seas. Biogeosciences 10, 6509–6544.
Clargo, N.M., Salt, L.A., Thomas, H., d. Baar, H.J.W., 2015. Rapid increase of observed DIC and pCO2 in the surface waters of the North Sea in the 2001–2011 decade ascribed to climate change superimposed by biological processes. Mar. Chem. 177, 566–581.
Colebrook, J.M., 1979. Continuous Plankton Records: Seasonal cycles of phytoplankton and copepods in the North Atlantic Ocean and North Sea. Mar. Biol. 51, 23–32.
Colebrook, J.M., Robinson, G.A., 1965. Continuous plankton records: seasonal cycles of phytoplankton and copepods in the north-eastern Atlantic and North Sea. Bull. Mar. Ecol. 6, 123–139.
Davis, C.E., Mahaffey, C., Wolff, G.A., Sharples, J., 2014. A storm in a shelf sea: variation in phosphorous distribution and organic matter stoichiometry. Geophys. Res. Lett. 41, 8452–8459. http://dx.doi.org/10.1002/2014GL061949.
de Boyer Montegut, C., Madec, G., Fischer, A.S., Lazar, A., Ludicone, D., 2004. Mixed layer depth over the global ocean: an examination of profile data and a profile-based climatology. J. Geophys. Res. 109, C12003. http://dx.doi.org/10.11029/12004JC002378.
de Haas, H., van Weering, T.C.E., de Stigter, H., 2002. Organic carbon in shelf seas: sinks or sources, processes and products. Cont. Shelf Res. 22, 691–717.
Dickson, A.G., Sabine, C.L., Christian, J.R., 2007. Guide to Best Practices for Ocean CO_2 Measurements, vol. 3. PICES Special Publication, 191p.
Dickson, R.R., Gould, W.J., Griffiths, C., Medler, K.J., Gmitrowicz, E.M., 1986. Seasonality in currents in the Rockall Channel. Proc. R. Soc. Edinb. 88B, 103–125.
Ducklow, H.W., McCallister, S.L., 2004. The biogeochemistry of carbon dioxide in the coastal oceans. In: Robinson, A.R., McCarthy, J., Rothschild, B.J. (Eds.), The Sea, vol. 13. pp. 269–315.
Egge, J.K., Asknes, D.L., 1992. Silicate as regulating nutrient in phytoplankton competition. Mar. Ecol. Prog. Ser. 83, 281–289.
Elrifi, I.R., Turpin, D.H., 1985. Steady-state luxury consumption and the concept of optimum nutrient ratios: a study with phosphate and nitrate limited *Selenastrum minutum* (Chlorophyta). J. Phycol. 21, 592–602.
Eppley, R.W., Rogers, J.N., McCarthy, J.J., 1969. Half-saturation constants for uptake of nitrate and ammonium by marine phytoplankton. Limnol. Oceanogr. 14, 912–919.
Falkowski, P.G., Biscaye, P.E., Sancetta, C., 1994. The lateral flux of biogenic particles from the eastern North American continental margin to the North Atlantic Ocean. Deep Sea Res. Part II 41 (2/3), 583–601.
Falkowski, P.G., Flagg, C.N., Rowe, G.T., Smith, S.L., Whitledge, T.E., Wirick, C.D., 1988. The fate of a spring phytoplankton bloom: export or oxidation? Cont. Shelf Res. 8 (5–7), 457–484.
Fehling, J., Davidson, K., Bolch, C.J.S., Brand, T.D., Narayanaswamy, B.E., 2012. The Relationship between Phytoplankton Distribution and Water Column Characteristics in North West European Shelf Sea Waters. PLoS ONE 7 (3), e34098.
Fouilland, E., Gosselin, M., Rivkin, R.B., Vasseur, C., Mostajir, B., 2007. Nitrogen uptake by heterotrophic bacteria and phytoplankton in Arctic surface waters. J. Plankton Res. 29 (4), 369–376.
Frigstad, H., Andersen, T., Hessen, D.O., Naustvoll, L.-J., Johnsen, T.M., Bellerby, R.G.J., 2011. Seasonal variation in marine C:N:P stoichiometry: can the composition of seston explain stable Redfield ratios? Biogeosciences 8, 2917–2933.
Geider, R., La Roche, J., 2002. Redfield revisited: variability of C:N:P in marine microalgae and its biochemical basis. Eur. J. Phycol. 37 (1), 1–17. http://dx.doi.org/10.1017/S0967026201003456.
Gilpin, L.C., Davidson, K., Roberts, E., 2004. The influence of changes in nitrogen:silicon ratios on diatom growth dynamics. J. Sea Res. 51, 21–35.
Grant, S.R., Bienfang, P.K., Laws, E.A., 2013. Steady-state bioassay approach applied to phosphate-limited continuous cultures: a growth study of the marine chlorophyte *Dunaliella salina*. Limnol. Oceanogr. 58 (1), 314–324.
Green, D.R.H., Cooper, M.J., German, C.R., Wilson, P.A., 2003. Optimization of an inductively coupled plasma - optical emission spectrometry method for the rapid determination of high-precision Mg/Ca and Sr/Ca in foraminiferal calcite. Geochem. Geophys. Geosyst. 4 (6), 8404. http://dx.doi.org/10.1029/2002GC000488.
Hartman, S.E., Kivimae, C., Salt, L., Clargo, N.M., 2017. Dissolved Inorganic Carbon and Total Alkalinity from cruise DY017 to the Hebrides Shelf (55–60°N, 6–10°W). British Oceanographic Data Centre - Natural Environment Research Council, UK. doi:10/b83q.
Hillebrand, H., Steinert, G., Boersma, M., Malzahn, A., Meunier, C.L., Plum, C., Ptacnik, R., 2013. Goldman revisited: faster-growing phytoplankton has lower N:P and lower stoichiometric flexibility. Limnol. Oceanogr. 58 (6), 2076–2088.
Holt, J., Wakelin, S., Huthnance, J., 2009. Down-welling circulation of the northwest European continental shelf: a driving mechanism for the continental shelf carbon pump. Geophys. Res. Lett. 36, L14602. http://dx.doi.org/10.11029/12009GL038997.
Hopkinson, C.S., Vallino, J.J., 2005. Efficient export of carbon to the deep ocean through dissolved organic matter. Nature 433, 142–145.
Hopkinson Jr, C.S., Vallino, J.J., Nolin, A., 2002. Decomposition of dissolved organic matter from the continental margin. Deep-Sea Res. II 49, 4461–4478.
Hopkinson Jr., C.S., Fry, B., Nolin, A.L., 1997. Stoichiometry of dissolved organic matter dynamics on the continental shelf of the northeastern U.S.A. Continent. Shelf Res. 17(5), 473–489.
Hung, J.-J., Chen, C.-H., Gong, G.-C., Sheu, D.-D., Shiah, F.-K., 2003. Distributions, stoichiometric patterns and cross-shelf exports of dissolved organic matter in the East China Sea. Deep Sea Res. Part II 50, 1127–1145.
Huthnance, J.M., 1986. The Rockall slope current and shelf-edge processes. Proc. R. Soc. Edinb. 88B, 83–101.
Huthnance, J.M., Holt, J.T., Wakelin, S.L., 2009. Deep ocean exchange with west-European shelf seas. Ocean Sci. 5, 621–634.
Hydes, D.J., Le Gall, A.C., Miller, A.E.J., Brockmann, U., Raabe, T., Holley, S., Alvarez-Salgado, X., Antia, A., Balzer, W., Chou, L., Elskens, M., Helder, W., Joint, I., Orren, M., 2001. Supply and demand of nutrients and dissolved organic matter at and across the NW European shelf break in relation to hydrography and biogeochemical activity. Deep-Sea Res. II 48, 3023–3047.
Hydes, D.J., Aoyama, M., Aminot, A., Bakker, K., Becker, S., Coverly, S., Daniel, A., Dickson, A.G., Grosso, O., Kerouel, R., van Ooijen, J., Sato, K., Tanhua, T., Woodward, E.M.S., Zhang, J.Z., 2010. Determination of dissolved nutrients (N, P, Si) in seawater with high precision and inter-comparability using gas-segmented continuous flow analysers. The GO-Ship Repeat Hydrography Manual: A collection of expert reports and guidelines, IOCCP Report No. 14, ICPO Publication Series No. 134. Version 1, 2010, pp. 1–87.
Joint, I., Wollast, R., Chou, L., Batten, S., Elskens, M., Edwards, E., Hirst, A., Burkill, P., Groom, S., Gibb, S., Miller, A., Hydes, D., Dehairs, F., Antia, A., Barlow, R., Reesa, A., Pomroy, A., Brockmann, U., Cummings, D., Lampitt, R., Loijens, M., Mantoura, F., Miller, P., Raabe, T., Alvarez-Salgado, X., Stelfox, C., Woolfenden, J., 2001. Pelagic production at the Celtic Sea shelf break. Deep-Sea Res. II 48, 3049–3081.
Joint, I.R., Pomroy, A.J., 1987. Activity of heterotrophic bacteria in the euphotic zone of the Celtic Sea. Mar. Ecol. Prog. Ser. 41, 155–165.
Kepkay, P.E., Niven, S.E.H., Milligan, T.G., 1993. Low molecular weight and colloidal DOC production during a phytoplankton bloom. Mar. Ecol. Prog. Ser. 100, 233–244.
Kirkwood, D.S., 1996. Nutrients: Practical notes on their determination in seawater. ICES Techniques in Marine Environmental Sciences Report 17. International Council for the Exploration of the Seas, Copenhagen, 25p.
Kirchman, D.L., 1994. The uptake of inorganic nutrients by heterotrophic bacteria. Microb. Ecol. 28, 255–271.
Kirchman, D.L., 2000. Uptake and regeneration of inorganic nutrients by marine heterotrophic bacteria. In: Kirchman, D.L. (Ed.), Microbial Ecology of the Ocean. Wiley-Liss, New York, pp. 261–288.
Lancelot, C., Billen, G., 1985. Carbon-nitrogen relationships in nutrient metabolism of coastal marine ecosystems. Adv. Aquat. Microbiol. 3, 263–321.
Langdon, C., 2010. Determination of dissolved oxygen in seawater by Winkler titration using the amperometric technique. The GO-Ship Repeat Hydrography Manual: a collection of expert reports and guidelines, IOCCP Report No. 14, ICPO Publication Series No. 134. Version 1, 2010, pp. 1–18.
Laruelle, G.G., Lauerwald, R., Pfeil, B., Regnier, P., 2014. Regionalized global budget of the CO_2 exchange at the air-water interface in continental shelf seas. Global Biogeochem. Cycles 28, 1199–1214. http://dx.doi.org/10.1002/2014GB004832.
Laws, E.A., Pei, S.F., Bienfang, P., Grant, S., Sunda, W.G., 2011. Phosphate-limited growth of *Pavlova lutheri* (Prymnesiophyceae) in continuous culture: determination of growth-rate-limiting substrate concentrations with a sensitive bioassay procedure. J. Phycol. 47, 1089–1097. http://dx.doi.org/10.1111/j.1529-8817.2011.01040.x.
Leeks, G.J.L., Jarvie, H.P., 1998. Introduction to the Land-Ocean Interaction Study (LOIS): rationale and international context. Sci. Total Environ. 210–211, 5–20.
Leonardos, N., Geider, R.J., 2004. Effects of nitrate:phosphate supply ratio and irradiance on the C:N:P stoichiometry of *Chaetoceros muelleri*. Eur. J. Phycol. 39, 173–180.
Liu, K.-K., Atkinson, L., Quinones, R., Talaue-McManus, L., 2010. Carbon and nutrient fluxes in continental margins. Springer-Verlag, Berlin.
LOIS-SES Project Members, 1999. Shelf Edge Study project dataset (1995–1996). Natural Environmental Research Council published by British Oceanographic Data Center. Bidston Observatory, Birkenhead, Merseyside (3 CD-ROM).
Lønborg, C., Davidson, K., Alvarez-Salgado, X.A., Miller, A.E.J., 2009. Bioavailability and bacterial degradation rates of dissolved organic matter in a temperate coastal area during an annual cycle. Mar. Chem. 113, 219–226.
Lønborg, C., Alvarez-Salgado, X.A., 2012. Recycling versus export of bioavailable dissolved organic matter in the coastal ocean and efficiency of the continental shelf pump. Global Biogeochem. Cycles 26, GB3018. http://dx.doi.org/10.1029/2012GB004353.
Mackenzie, F.T., Andersson, A., Lerman, A., Ver, L.M., 2004. Boundary exchanges in the global coastal margin: implications for the organic and inorganic carbon cycles. In: Robinson, A.R., Brink, K.H. (Eds.), The Sea, vol. 13. Harvard University Press, pp. 193–225.

Martiny, A.C., Vrugt, J.A., Lomas, M.W., 2014. Concentrations and ratios of particulate organic carbon, nitrogen, and phosphorus in the global ocean. Scientific Data 1, 140048. http://dx.doi.org/10.141038/sdata.142014.140048.

Martiny, A.C., Vrugt, J.A., Primeau, F.W., Lomas, M.W., 2013. Regional variation in the particulate organic carbon to nitrogen ratio in the surface ocean. Global Biogeochem. Cycles 27, 723–731. http://dx.doi.org/10.1002/gbc.20061.

McCubbin, D., Leonard, K.S., Brown, J., Kershaw, P.J., Bonfield, R.A., Peak, T., 2002. Further studies of the distribution of technetium-99 and caesium-137 in UK and European coastal waters. Cont. Shelf Res. 22, 1417–1445.

McKay, W.A., Baxter, J.M., Ellett, D.J., Meldrum, D.T., 1986. Radiocaesium and circulation patterns west of Scotland. J. Environ. Radioact. 4, 205–232.

Mitchell, L., Harvey, S.M., Gage, J.D., Fallick, A.E., 1997. Organic carbon dynamics in shelf edge sediments off the Hebrides: a seasonal perspective. Int. Rev. Gesamten Hydrobiol. 82, 425–435.

Moschonas, G., Gowen, R.J., Stewart, B.M., Davidson, K., 2015. Nitrogen dynamics in the Irish Sea and adjacent shelf waters: an exploration of dissolved organic nitrogen. Estuar. Coast. Shelf Sci. 164, 276–287.

Muller-Karger, F.E., Varela, R., Thunell, R., Luerssen, R., Hu, C., Walsh, J.J., 2005. The importance of continental margins in the global carbon cycle. Geophys. Res. Lett. 32, L01602. http://dx.doi.org/10.01029/02004GL021346.

Officer, C.B., Ryther, J.H., 1980. The possible importance of silicon in marine eutrophication. Mar. Ecol. Prog. Ser. 3, 83–91.

OMEX Project Members, 1997. Ocean Margin Exchange, OMEX-I project dataset (1993–1996). Natural Environmental Research Council published by British Oceanographic Data Center. Bidston Observatory, Birkenhead, Merseyside (2 CD-ROM), hdl:10013/epic.28817.d001.

Painter, S., 2017. Particulate measurements from CTD niskin collected depth profiles conducted during cruise DY017 to the Hebrides Shelf (55–60°N, 6–10°W). British Oceanographic Data Centre - Natural Environment Research Council, UK. doi:10/b83r.

Painter, S.C., Henson, S.A., Forryan, A., Steigenberger, S., Klar, J., Stinchcombe, M.C., Rogan, N., Baker, A.R., Achterberg, E.P., Moore, C.M., 2014. An assessment of the vertical diffusive flux of iron and other nutrients to the surface waters of the subpolar North Atlantic Ocean. Biogeosciences 11, 2113–2130.

Painter, S.C., Hartman, S.E., Kivimäe, C., Salt, L.A., Clargo, N.M., Bozec, Y., Daniels, C.J., Jones, S.C., Hemsley, V.S., Munns, L.R., Allen, S.R., 2016. Carbon exchange between a shelf sea and the ocean: the Hebrides Shelf, west of Scotland. J. Geophys. Res. 121, 4522–4544. http://dx.doi.org/10.1002/2015JC011599.

Prandle, D., 1984. A modelling study of the mixing of ^{137}Cs in the seas of the European Continental Shelf. Philos. Trans. R. Soc. A 310, 407–436.

Ptacnik, R., Andersen, T., Tamminen, T., 2010. Performance of the Redfield Ratio and a family of nutrient limitation indicators as thresholds for phytoplankton N vs P limitation. Ecology 13, 1201–1214.

Ragueneau, O., Treguer, P., 1994. Determination of biogenic silica in coastal waters: applicability and limits of the alkaline digestion method. Mar. Chem. 45, 43–51.

Raimbault, P., Diaz, F., Pouvesle, W., Boudjellal, B., 1999. Simultaneous determination of particulate organic carbon, nitrogen and phosphorous collected on filters, using a semi-automatic wet-oxidation method. Mar. Ecol. Prog. Ser. 180, 289–295.

Redfield, A.C., Ketchum, B.H., Richards, F.A., 1963. The influence of organisms on the composition of sea-water. In: Hill, M.N. (Ed.), The Sea: Vol 2: Composition of Seawater Comparative and Descriptive Oceanography. Interscience, London, pp. 26–77.

Regnier, P., Friedlingstein, P., Ciais, P., Mackenzie, F.T., Gruber, N., Janssens, I.A., Laruelle, G.G., Lauerwald, R., Luyssaert, S., Andersson, A.J., Arndt, S., Arnosti, C., Borges, A.V., Dale, A.W., Gallego-Sala, A., Goddéris, Y., Goossens, N., Hartmann, J., Heinze, C., Ilyina, T., Joos, F., LaRowe, D.E., Leifeld, J., Meysman, F.J.R., Munhoven, G., Raymond, P.A., Spahni, R., Suntharalingam, P., Thullner, M., 2013. Anthropogenic perturbation of the carbon fluxes from land to ocean. Nat. Geosci. 6, 597–606.

Riegman, R., Stolte, W., Noordeloos, A.A.M., Slezak, D., 2000. Nutrient uptake, and alkaline phosphate (EC 3:1:3:1) activity of *Emiliania huxleyi* (Prymnesiophyceae) during growth under N and P limitation in continuous cultures. J. Phycol. 36, 87–96. http://dx.doi.org/10.1046/j.1529-8817.2000.99023x.

Robinson, G.A., 1970. Continuous plankton records: variation in the seasonal cycle of phytoplankton in the North Atlantic. Bull. Mar. Ecol. 6, 333–345.

Schlesinger, W.H., Bernhardt, E.S., 2013. Biogeochemistry: An Analysis of Global Change, third ed. Academic Press, Amsterdam, 672p.

Sharples, J., 2010. Subpolar margins. In: Liu, K.K., Atkinson, L., Quiñones, R., Talaue-McManus, L. (Eds.), Carbon and Nutrient Fluxes in Continental Margins. Springer-Verlag, Berlin Heidelberg, pp. 211–215.

Siemering, B., Bresnan, E., Painter, S.C., Daniels, C.J., Inall, M., Davidson, K., 2016. Phytoplankton distribution in relation to environmental drivers on the North West European shelf sea. PLoS ONE 11 (10), e0164482. http://dx.doi.org/10.0161371/journal.pone.0164482.

Simpson, J.H., McCandliss, R.R., 2013. "The Ekman Drain": a conduit to the deep ocean for shelf material. Ocean Dyn. 63, 1063–1072.

Simpson, J.H., Sharples, J., 2012. Introduction to the Physical and Biological Oceanography of Shelf Seas. Cambridge University Press, UK, Cambridge, pp. 424.

Smith, S.V., Hollibaugh, J.T., 1993. Coastal metabolism and the oceanic organic carbon balance. Rev. Geophys. 31 (1), 75–89.

Souza, A.J., Simpson, J.H., Harikrishnan, M., Malarkey, J., 2001. Flow structure and seasonality in the Hebridean slope current. Oceanologica Acta 24(Suppl.), S63–S76.

Sterner, R.W., Elser, J.J., 2002. Ecological Stoichiometry. Princeton University Press, New Jersey, pp. 439.

Sterner, R.W., Andersen, T., Elser, J.J., Hessen, D.O., Hood, J.M., McCauley, E., Urabe, J., 2008. Scale-dependent carbon: nitrogen: phosphorous seston stoichiometry in marine and freshwaters. Limnol. Oceanogr. 53 (3), 1169–1180.

Testa, J.M., Kemp, W.M., 2011. Oxygen - dynamics and biological consequences. In: Wolanski, E., McLusky, D. (Eds.), Treatsie on Estuarine and Coastal Science. Academic Press, pp. 163–199.

Tett, P., Hydes, D., Sanders, R., 2003. Influence of nutrient biogeochemistry on the ecology of northwest European shelf seas. In: Black, K.D., Shimmield, G.B. (Eds.), Biogechemistry of Marine Systems. Blackwell Publishing, Sheffield, pp. 294–363.

Thomas, H., 2002. Remineralization ratios of carbon, nutrients, and oxygen in the North Atlantic Ocean: a field databased assessment. Global Biogeochem. Cycles 16 (3), 1051. http://dx.doi.org/10.1029/2001GB001452.

Thomas, H., Bozec, Y., de Baar, H.J.W., Elkalay, K., Frankignouelle, M., Schiettecatte, L.-S., Kattner, G., Borges, A.V., 2005. The carbon budget of the North Sea. Biogeosciences 2, 87–96.

Thomas, H.E., Bozec, Y., Elkalay, K., De Baar, H.J.W., 2004. Enhanced open ocean storage of CO_2 from shelf sea pumping. Science 304, 1005–1008.

Thrane, J.-E., Hessen, D.O., Andersen, T., 2016. The impact of irradiance on optimal and cellular nitrogen to phosphorus ratios in phytoplankton. Ecol. Lett. 19 (8), 880–888.

Thrane, J.-E., Hessen, D.O., Andersen, T., 2017. Plasticity in algal stoichiometry: experimental evidence of a temperature-induced shift in optimal supply N:P ratio. Limnol. Oceanogr. http://dx.doi.org/10.1002/lno.10500.

Topcu, H.D., Brockmann, U.H., 2015. Seasonal oxygen depeletion in the North Sea, a review. Mar. Pollut. Bull. 99, 5–27.

Wakelin, S.L., Holt, J.T., Blackford, J.C., Allen, J.I., Butenschon, M., Artioli, Y., 2012. Modeling the carbon fluxes of the northwest European continental shelf: validation and budgets. J. Geophys. Res. 117, C05020. http://dx.doi.org/10.01029/02011JC007402.

Williams l, P.J., 1995. Evidence for the seasonal accumulation of carbon-rich dissolved organic matter, its scale in comparison with changes in particulate material and the consequential effect on net C/N assimilation ratios. Mar. Chem. 51, 17–29.

Wollast, R., 1998. Evacuation and comparison of the global carbon cycle in the coastal zone and in the open ocean. In: Brink, K., Robinson, A.R. (Eds.), The Sea, vol. 10. Wiley, New York, pp. 213–252.

Wong, P.P., Losada, I.J., Gattuso, J.-P., Hinkel, J., Khattabi, A., McInnes, K.L., Saito, Y., Sallenger, A., 2014. Coastal Systems and Low-Lying Areas. In: Field,C.B., Barros, V.R., Dokken, D.J., Mach, K.J., Mastrandrea, M.D., Bilir, T.E., Chatterjee, M., Ebi, K.L., Estrada, Y.O., Genova, R.C., Girma, B., Kissel, E.S., Levy, A.N., MacCraken, S., Mastrandrea, P.R., White, L.L. (Eds.), Climate Change 2014: Impacts, Adaptation, and Vulnerability. Part A: Global and Sectoral Aspects. Contribution of Working Group II to the Fifth Assessment Report of the Intergovernmental Panel on Climate Change. Cambridge University Press, Cambridge, UK & New York, USA, pp. 361–409.

Xu, W., Miller, P.I., Quartly, G.D., Pingree, R.D., 2015. Seasonality and interannual variability of the European Slope current from 20 years of altimeter data compared with in situ measurements. Remote Sens. Environ. 162, 196–207.